Time synchronization of spindles and slow wave oscillation in nocturnal EEG

Katja Törmä
Master's thesis
University of Eastern Finland
Faculty of Science and Forestry
Department of Applied Physics
24. kesäkuuta 2024

UNIVERSITY OF EASTERN FINLAND, Faculty of Science and Forestry
Master of Science Programme in Applied Physics, Medical Physics
Törmä, Katja, B.Sc.; Master's thesis, 42 pages
Supervisors: Henna Pitkänen, M.Sc., Henri Korkalainen, Ph.D.
June 2024

Keywords: sleep spindle, slow wave, electroencephalography, time synchronization

Abstract

The time synchronization of sleep spindles and slow wave oscillation in electroencephalogram (EEG) signal has been increasing in interest due to their possible link to processes such as memory consolidation and forgetting. However, considering the amount of different tools that have been used for pattern detection and analysis of time synchronization (e.g. wavelet transforms, correlation histograms), it is essential to be aware of the differences between the methodologies behind these tools and the possible effect of the different methods on the obtained results. Therefore, the main objective of this thesis was to compare the time synchronization results from complex demodulation and the Hilbert transform and to analyze possible differences between these methodologies. Furthermore, time synchronization of spindles and slow waves can be studied from two approaches; either by detecting spindles related to the slow waves or vice versa. Both of these approaches were considered in the analyses.

The study was performed on EEG-signals obtained from overnight polysomnographies of 899 patients with suspected sleep apnea. To utilize both of aforementioned approaches, two separate datasets were formed in the study. The first dataset was obtained by detecting and position-locking slow waves from the sleep EEG. The second dataset was obtained by identifying spindles from the same EEG-segments, using an algorithm based on the combination of the empirical mode decomposition (EMD) and the continuous wavelet transform (CWT), and position-locking the spindles. Thus, the two datasets were formed from the same EEG-signal segments, but in the first dataset the segments were position-locked according to the slow waves and in the second dataset according to the spindles. For both of these datasets separately, the Hilbert transform and complex demodulation were performed to study the time synchronization, and the results from these methods were compared.

Time synchronization between slow waves and sleep spindles was observed using both the Hilbert transform and complex demodulation. Specifically, the strongest coupling of the spindles and slow waves was observed with both methods at the ascending slope of the slow wave, close to the positive peak of the slow wave, and at the positive peak. Another location where coupling was detected was at the descending slope of the slow wave. The aforementioned results were found in both datasets when using the Hilbert transform and complex demodulation. In conclusion, both Hilbert transform and complex demodulation were observed to produce similar results. Thus, both methods were concluded to be equally sufficient to study the time synchronization of sleep spindles and slow waves.

Tiivistelmä

Unenaikaisesta aivosähkökäyrästä (*electroencephalogram*, EEG) havaittavien hidasaaltojen ja unisukkuloiden aikasynkronisaatiota on tutkittu lähivuosina runsaasti johtuen aikasynkronisaation mahdollisesta yhteydestä aivoissa tapahtuviin prosesseihin, kuten muistin vahvistamiseen sekä unohtamiseen. EEG:n hidasaaltojen ja unisukkuloiden välistä aikasynkronisaatiota on myös tutkittu usealla eri menetelmällä, kuten aallokemuunnoksilla tai korrelaatiohistogrammeilla. Eri menetelmiä käytettäessä on kuitenkin tärkeää ottaa huomioon niiden mahdollinen vaikutus saatuihin tuloksiin Täten tässä tutkielmassa on vertailtiin kahden eri aikasynkronisaatiomenetelmän; Hilbertin muunnoksen ja kompleksisen demodulaation tuloksia. Erilaisten menetelmien käyttämisen lisäksi aikasynkronisaatiota on tutkittu kahdesta eri lähestymiskulmasta: joko tarkastelemalla hidaasaaltojen yhteydessä esiintyviä unisukkuloita tai unisukkuloiden yhteydessä esiintyviä hidasaaltoja. Täten tässä tutkielmassa huomioitiin molemmat lähestymistavat.

Lähestymistapoja tutkittiin EEG-signaaleista, jotka oli kerätty 899 potilaalta unipolygrafiatutkimuksen yhteydessä uniapneaepäilyn vuoksi. Tutkimuksessa rekisteröinneistä muodostettiin kaksi eri tietoaineistoa. Ensimmäinen koostui EEG-pätkistä, jotka sisälsivät paikannetut hidasaallot. Näistä EEG-pätkistä havainnointiin edelleen unisukkulat käyttämällä algoritmia, jossa yhdistettiin empiirinen tyyppiarvohajotelma (*empirical mode decomposition*, EMD) ja jatkuva aaltomuunnos (*continuous wavelet transform*, CWT). Ensimmäisessä aineistossa edellämainitut EEG-segmentit paikkalukittiin niiden sisältämien hidasaaltojen pienimmän amplitudin mukaan ja toisessa aineistossa samat EEG-pätkät paikkalukittiin niistä havaittujen spindlejen suurimman amplitudin mukaan. Näiden kahden tietoaineiston aaltomuotojen aikasynkronisaatiota tutkittiin Hilbertin muunnoksen ja kompleksisen demodulaation avulla.

Hidasaaltojen ja unisukkuloiden aikasykronisaatiota havaittiin sekä Hilbertin muunnoksella että kompleksisella demodulaatiolla siten, että molempien menetelmien havainnot tukivat toisiaan. Vahvin aikasynkronisaatio havaittiin hidasaallon nousevalla käyrällä ennen hidasaallon positiivista huippua sekä positiivisella huipulla. Myös hidasaallon laskevalla käyrällä havaittiin aikasynkronisaatiota. Edellämainitut tulokset havaittiin molempien menetelmien lisäksi myös molemmissa tietoaineistoissa. Täten molemmat menetelmät tuottivat vastaavat tulokset ja molempien menetelmien havaittiin olevan riittäviä unisukkuloiden ja hidasaaltojen aikasynkronisaation tutkimisessa.

Contents

1 Introduction

Sleep has been a subject of interest for centuries and cures for sleep disorders such as insomnia can be traced back to ancient Egypt [1]. In ancient Greece, Aristotle attempted to explain the phenomenon of sleep and waking as well as the relationship between sleep and food [1]. Additionally, ancient Chinese medicine offered solutions, such as acupuncture, for sleep disorders [1]. In the western world, France and Italy took steps to understand sleep in the Middle Ages, and in the 17th century Thomas Willis was able to describe narcolepsy and restless leg syndrome [1]. In the 19th century the amount of studies on sleep increased and circadian rhythms as well as body temperature changes related to sleep were studied [1].

However, the most notable steps in the field of sleep studies were taken in the 20th century [1]. One of these steps was taken by a German psychiatrist Hans Berger, who was able to extract an electrical waveform from measured brain activity, called alpha rhythm, and is considered to be the father of electroencephalography (EEG) [2]. However, Berger was not the first to study the electrical activity of the brain. Instead, in 1874 a Scottish physiologist Richard Canton had published studies on rabbit and monkey brains, where he observed that applying light to the eye would result in strong current fluctuations in the cerebral cortex [3]. Subsequently, in 1935 Alfred Lee Loomis conducted measurements on human subjects while they were sleeping [4]. Loomis et al. would play sounds to the sleeping subjects and as a result they recorded "trains of rhythmic potential changes" [4]. In the later decades of the 20th century, the studies continued on EEG recordings and in 1968 a manual for the analysis of sleep recordings was released by Allan Rechtschaffen and Anthony Kales: A Manual of Standardized Terminology, Techniques and Scoring System for Sleep Stages of Human Subjects [5]. This manual gave common rules for staging the sleep recordings, i.e., dividing the sleep into segments of light, deep or rapid eye movement sleep based on the characteristics of the recorded signals [1]. Later, in 2007 the American Academy of Sleep Medicine (AASM) proposed new scoring definitions to replace the previous R&K rules [6]. Since then, the AASM guidelines have been updated and remained to be the standard in clinical practice [7].

Nowadays, sleep research is more widespread, not just focusing on adults but adolescents and children as well [8, 9, 10]. Studies have concluded that humans spend approximately 25 years of their lives sleeping [11] and insufficient sleep can lead to a decrease in cognitive performance [12] as well as an increased risk in mortality [13]. Decreased amount of sleep has also been linked with diseases such as cancer, cardiovascular disease, and obesity [13]. Therefore, studying and understanding sleep disorders, which can seriously alter the quality and the length of sleep, is vital. However, despite all advances in sleep research, a lot still remains to be discovered on the purpose of sleep [14]. The current perspective focuses on sleep being a restorative process, however, it is still unclear where this restoration extends [11].

The work on sleep EEG has lead to the discovery of several patterns in the signals such as K-complexes, sleep spindles, parahippocampal ripples, and slow waves [15, 16]. These patterns and their possible synchronization with each other has been a subject of interest due to their possible link to processes such as memory consolidation and forgetting [17].

Historically, sleep waveforms such as sleep spindles have been detected visually by a trained technician, however due to intra- and interscorer variabilities and the laborious effort required by visual detection, new more automated approaches have been developed [18]. Over the years, several analyzing methods have been implemented in the detection of sleep waveforms [19, 20, 21, 22] and the amount of methods is constantly increasing. However, considering the amount of different tools that can be chosen for pattern detection and analysis, it can be overwhelming to decide which approach may be the most suitable for a certain application. Therefore, it can be useful to compare different methods and their results to understand their benefits and disadvantages in regards to the chosen application.

Furthermore, time synchronization between sleep spindles and slow wave oscillation has been observed in previous studies [17, 23, 24, 25, 26]. However, these studies have utilized several different methods in the detection of sleep spindles and the time synchronization between spindles and slow waves. Therefore, comparing results obtained by different methods can give more insight on how to choose a method for these studies and which methodology would suit each purpose the best. In this thesis I present my results on sleep spindle and slow wave time synchronization utilizing two different analyzing methods. Both methods were first conducted from the perspective of the slow waves and then from the perspective of the spindles. This was done for the purpose of studying whether the chosen approach has an impact on the results. The analyzing methods investigated in this thesis study are complex demodulation and Hilbert transform.

2 Electroencephalography

EEG is a measurement method utilized to obtain a biosignal originating from the electrical activity in the brain [27]. The electrical activity of the brain is generated in nerve cells in the form of action potentials [28]. The action potential is generated when the membrane potential of the nerve cell rises from approximately -70 mV to -50 mV due to excitatory stimulus [29]. This will lead to changes in the membrane permeabilities for sodium (Na^+) and potassium (K^+) ions [29]. Due to increased permeability, sodium ions flow inside the nerve cell, resulting in increased potential inside the nerve cell [28]. During this event, also referred to as depolarization, the potential inside the nerve cell can increase up to 20 mV [28]. The depolarization phase of the action potential will end when the sodium ion channels close automatically [28].

After the depolarization phase, the potassium ion permeability, which is voltage dependent, increases and results in a slow efflux of potassium ions [28]. The efflux of potassium ions will restore the membrane potential of the nerve cell back to resting potential [29]. This event is also referred to as repolarisation [29].

After the action potential has been generated in the nerve cell, it will propagate along the axon of the nerve cell [29]. However, the action potentials itself are not high enough in extracellular amplitude and in duration (approximately 1 ms) to be recorded [28]. Instead, postsynaptic potentials have a longer duration (over 10 ms) and therefore, the summation of several simultaneous and parallel postsynaptic potentials of pyramidal nerve cells can be recorded from the scalp as EEG [28]. More specifically, EEG is considered to measure the extracellular currents of activated nerve cells [27]. The postsynaptic potentials can be either excitatory postsynaptic potentials (EPSP) or inhibitory postsynaptic potentials (IPSP) [28]. With EPSP, the neurotransmitters are excitatory and them binding to neurotransmitter receptors result in positive voltage at the postsynaptic membrane, i.e., depolarization [28]. Alternatively, IPSP is produced when inhibitory neurotransmitters binding to their receptors result in more negative voltage than the resting membrane voltage on the postsynaptic membrane, i.e., hyperpolarization [28].

To measure the brain activity, EEG electrodes are placed on the scalp according to the so-called 10-20 system [30]. In this standard electrode placement method, 21 electrodes are placed at "10% or 20% relative distances between the cranial landmarks" [31]. However, the number of channels used in EEG recordings can increase up to 256 in certain applications, which will require a higher density of electrodes [31]. Therefore, to enable repeatability between studies, other placement methods have been proposed to answer the demands of the increasing number of electrodes. One of the methods is the 10-10 system, which is an extension from 10-20 system and it replaces the 20% relative distance with 10% [31]. This extension has been accepted by the American Clinical Neurophysiological Society and the International Federation of Clinical Physiology [31].

EEG is the most used signal acquisition modality related to brain activity measurements due to it being relatively cost-effective, having good temporal resolution and portability as well as being safe to use [32]. Downside of EEG is that the signals are

non-stationary and the quality of the signals can be easily compromised by noise or other artefacts [33]. Even the mood or the posture of the subject can have an effect on the signal quality [33]. Furthermore, the source localization from EEG recordings can be challenging since the tissues surrounding the cortex, i.e., cerebrospinal fluid, skull, and skin have different electrical conductivities leading to low spatial resolution [27].

EEG has several applications in the medical field, for example in neurology with epilepsy, Parkinson's disease, and sleep disorders, as well as in neuroscience such as sleep research [30]. In disorders such as schizophrenia, the EEG signal recorded from the patient may have abnormalities [34]. Additionally, EEG has applications in neurogaming, brain-computer interfaces, and navigating robotic body parts, among others [30].

3 Sleep

Sleep is a fundamental part of human life. The reasons for sleep and dreaming are still debated, despite the increased knowledge on the neuroanatomy and -physiology over the past 50 years [11]. Currently the perspective is that sleep is "a highly organized state generated by the cooperative interplay of many behavioral and neural components" [11]. Studies have linked the importance of sleep to various bodily functions that are important to human health such as cardiovascular health, mental health, cognition, memory consolidation, immunity, reproductive health, and hormone regulation [35].

In normal human EEG, frequencies in the range of 1–30 Hz are recorded [11]. This frequency range can be further divided into four different frequency bands: delta (0.5–4 Hz), theta (4–7 Hz), alpha (8–13 Hz), and beta (13–30 Hz). The EEG measured during sleep can be evaluated based on the frequency content and specific characteristics of the signal such as sleep spindles and K-complexes [6]. According to the AASM, the sleep EEG can be scored, i.e., separated into four different stages [6]. These stages include three non-rapid eye movement (NREM) stages and one rapid eye movement (REM) stage. The NREM stages are scored in 30 s long segments, also referred to as epochs, as stage N1 (NREM 1), stage N2 (NREM 2) and stage N3 (NREM 3) [6]. During the stage N1, sleep is the lightest, during stage N2, it is slightly deeper and during stage N3 sleep is the deepest [36]. The sleep EEG typically consists of 90 minute cycles where all sleep stages are usually visible progressing from N1 to N2 to N3, and ending in REM sleep after which a new cycle begins [36]. The sleep stages form a graph called a hypnogram (Figure 1).

N1 is a sleep stage defined by low amplitude mixed frequency content in the EEG and slow eye movements (SEM) with length of >500 ms [6]. This sleep stage may also exhibit vertex sharp waves in the EEG signal [6].

The second NREM sleep stage, N2, can be scored when sleep spindles and K-complexes are observed in the EEG signal [6]. Sleep spindles often exhibit their highest amplitudes in central EEG channels [6]. K-complexes are sharp waveforms

which can be recognised from the EEG by observing a negative peak which is then followed by a positive peak with a total length of $\geq$0.5 s for the whole waveform [6]. K-complexes exhibit the highest amplitudes in the frontal EEG channels [6]. The background activity of EEG in N2 stage has a low amplitude and a variety of mixed frequencies [37].

Sleep stage N3 has been defined in the AASM scoring manual to consist of slow wave activity which refers to EEG waves in the frequency range of 0.5–2 Hz [6]. Additionally, the peak-to-peak amplitude should be higher than 75 µV when recorded over the frontal channels [6]. In N3 sleep spindles and K-complexes may occur but eye movements are not observed [37].

REM sleep stage is characterized by rapid eye movements and low chin electromyography (EMG) tone [6]. The rapid eye movements are maximally 500 ms long sharp deflections, observed in the electrooculography (EOG) signal [6]. Other phenomena observed in REM sleep stage are sawtooth waves in the EEG and transient muscle activity that can be seen in the EEG, EMG, or EOG signals [6]. Additionally, the baseline EEG signal has mixed frequency content as well as a low amplitude [6]. From a physiological perspective, REM sleep stage has been associated with dreaming [35].

Age plays a vast role in the amount and the quality of human sleep. Newborns sleep considerable amounts during the day, up to 16–18 hours and over 50% of the sleep is REM sleep [11]. When the child grows, the amount of sleep decreases, and by the time that they are 3 to 5 years old, the amount of sleep needed in a day is around 10 to 12 hours [11]. At this age, the deep sleep stage N3 is relevant while REM sleep is still prominent [11]. As the age increases, the amount of sleep decreases and sleep will become more fragmented [11]. Additionally, the risk for sleep disorders, such as insomnia and restless legs syndrome, becomes more prevalent with age [11].

The gold standard method of sleep recordings is type I polysomnography (PSG) [38], recorded in a specialized sleep laboratory. In type I PSG, several signals are recorded from the body and based on the recorded signals, possible diagnoses for sleep disorders can be made [38]. The PSG includes signals such as EEG, electrocardiography (ECG), EOG, EMG, nasal and oral airflow, blood oxygen saturation, and chest and abdominal movement [38]. EOG is a signal commonly recorded with two channels, one channel for each eye to record the movement of the eyes [38]. The reference electrode for these channels is usually at the mastoid. To record muscle activity during sleep, EMG signal is recorded from the chin and limbs [38]. Respiratory activity is measured with a nasal cannula to examine the nasal airflow and the pressure of the airflow [38]. Additionally, oral airflow can be taken into account with a combined nasal-oral measurement device [38]. Other measurements for detecting breathing are respiratory inductance plethysmography (RIP), which includes belts measuring the movement of the ribcage and abdomen [38]. In addition to directly monitoring respiration, the oxygen saturation of arterial blood is often recorded [38]. It can be measured with a pulse oximeter from the finger or the earlobes [38]. Moreover, possible snoring of the subject is recorded by a microphone [38]. Additionally, PSG studies are usually performed in sleep laboratories and therefore, the sleeping position of the subject is recorded on video [38].

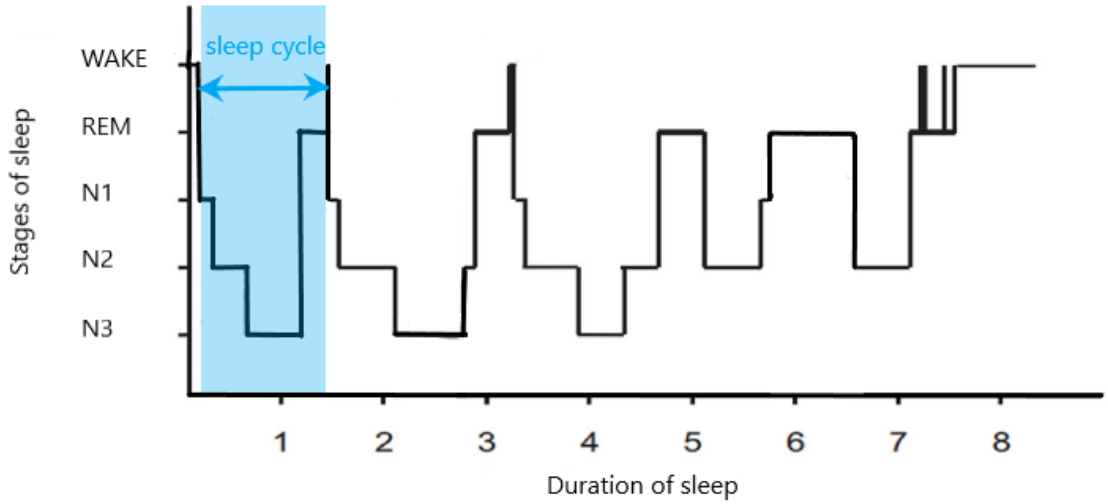

Figure 1: Example of a hypnogram, i.e., a scheme where all the sleep stages (wake, non-rapid eye movement (N1, N2, N3) and, rapid eye movement (REM)) have been scored for the duration of the whole night. One sleep cycle is determined when all the sleep stages from wake to deep sleep to REM sleep are visible in the hypnogram. Picture modified from [39].

3.1 Spindles

Sleep spindles were first separated from the EEG and named by Loomis et al. in 1935 [4]. Moreover, Hans Berger was involved in differentiating EEG rhythms [3]. In the AASM manual, spindles are defined as "a train of distinct waves with frequency of 11–16 Hz with duration of $\geq$0.5 s" (Figure 2) [6]. They can be detected from EEG signals in several channels [6].

Studies have shown that the 11–16 Hz spindle frequency range can be divided into two different groups depending on their frequency. Spindles with frequencies <13 Hz [40] or having their spectra centered around 12 Hz [41] are referred to as slow spindles [40] or low frequency spindles (LFS) [41] and spindles with frequencies >13 Hz [40] or having their spectra centered around 14 Hz [41] are referred to as fast spindles [40] or high frequency spindles (HFS) [41].

Sleep spindles are characteristic for N2 sleep stage but they can be observed during N3 sleep stage as well [37]. However, sleep spindles in N2 sleep stage tend to have a higher amplitude and occur more frequently compared to N3 sleep stage [40]. Furthermore, there is evidence to implicate that sleep spindles in N2 are primarily fast spindles and most of the spindles manifesting in N3 sleep stage are slow spindles [40]. Slow spindles can also occur in N2 but they tend to be smaller and they occur less frequently, while their location is not limited to parietal derivations only [40]. Additionally, fast spindles can be observed during N3 sleep stage, however they are typically observed in central EEG derivations [40].

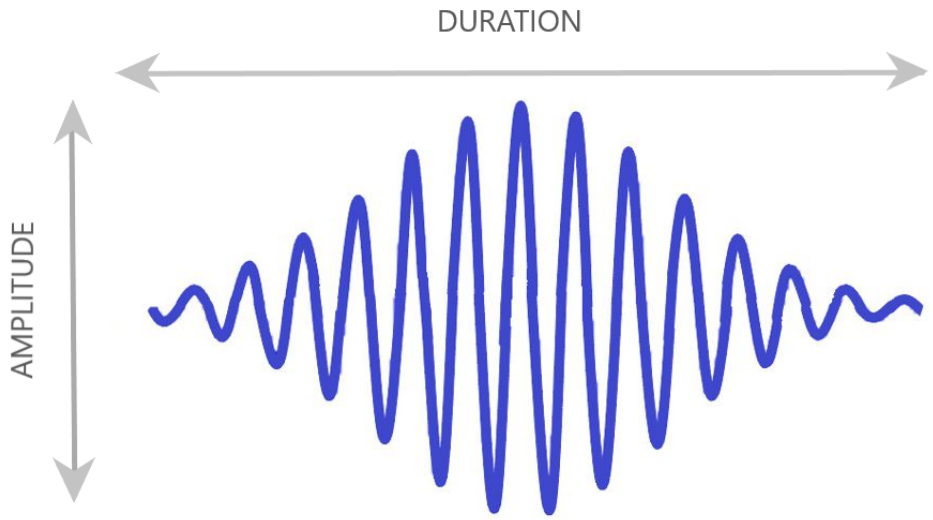

Figure 2: Sleep spindle is a train of oscillation in frequency of 11–16 Hz with a waxing and waning shape.

Some studies have associated sleep spindles with different disorders such as focal epilepsy and schizophrenia as well as Alzheimer's disease [17, 42, 43, 44]. In schizophrenia studies, spindle activity has been found to be diminished when compared to individuals without schizophrenia [43]. Furthermore, artificially increasing the amount of sleep spindles has been associated with improved cognition through memory consolidation [43]. Therefore, there is an interest to study whether increasing the amount of sleep spindles could be used as a treatment for patients with schizophrenia to improve their cognitive abilities [43]. Studies have also linked the absence of sleep spindles with an increased risk of mortality in Intensive Care Unit (ICU) patients [45]. Therefore, an interest remains to study sleep spindles as a potential biomarker for critically ill patients [45].

Already in 1950, fast and slow spindles were observed to originate from different parts of the brain [41, 46]. Gibbs et al. observed that LFS would occur mostly in the frontal recordings and HFS would be more prominent in the posterior derivations [46]. These findings have been confirmed by Jobert et al. [47] as well as Zygierewicz et al. [41]. Zygierewicz et al. found that LFS occur primarily in the frontal channels while HFS can be observed in the parietal channels [41]. They also observed that HFS would occur in a rhythmic manner with a period of 3.9 s while LFS showed no rhythmicity. Werth et al. concluded in their study that the origin of the sleep spindles included two functionally independent systems [48].

Despite the extensive research on the origin of sleep spindles, no consensus has been reached on which part of the brain is responsible for producing the sleep spindles. There are studies where sleep spindles have been shown to originate

from the thalamus [49] and it has been shown that the thalamic reticular nucleus (TRN) will continue generating spindle-related rhythms (7–16 Hz) even after being disconnected from other thalamic nuclei [50]. Therefore, TRN is also referred to as sleep spindle pacemaker [40]. According to this theory, a sleep spindle is formed when TRN generates rhythmic inhibitory synaptic potentials, as these inhibitory synaptic potentials have been detected being in phase with spindle waves [49].

However, studies done with EEG recordings support the idea that the origins of slow and fast spindles differ [40]. According to EEG measurements, the precuneus has been suggested to be the origin for fast spindles and prefrontal cortex has been linked with slow spindles [40]. Furthermore, studies done with magnetoencephalography (MEG) have indicated that there can be several sources for sleep spindles [40]. However, some results have shown that fast and slow spindles would originate from a common source but manifest successively [40]. This may indicate a presence of a single thalamic spindle generator which would produce one spindle that propagates in posterior-anterior direction [40]. Thus, despite the efforts, the origin of sleep spindles remains undetermined.

The standard method for detecting sleep spindles from sleep recordings is visual identification by trained technicians in sleep clinics [51]. Despite advances in automatic detection of sleep spindles, visual inspection by sleep technicians is still considered the gold standard [18]. However, relying only on visual inspection has its downsides. Variability has been reported between sleep experts, and more concealed spindles have been found difficult to detect due to background EEG activity [18, 51]. In these cases, automated detection methods can be efficient and consistent [18]. However, automated detection methods have their own disadvantages. Different automated detection methods tend to disagree more with each other than with visual detection [18]. Additionally, it may be difficult for the same automated detection method to consider the differences between spindle characteristics in older and younger populations [18].

There are various methods on how sleep spindles can be automatically detected from sleep EEG [40]. These methods can be divided into four categories: fixed thresholding, adaptive thresholding, time-frequency analysis, and machine learning techniques [40]. In fixed thresholding algorithms, the EEG signal is usually bandpass-filtered to spindle frequency range and then an amplitude criteria is added to detect the spindle [40]. Furthermore, a criteria for the length of the spindle is added as well [40]. This approach is quite inflexible since the amplitude is usually pre-set and it does not take into account spindle amplitude differences between subjects or EEG-channels [40]. Therefore, utilizing the same algorithm for a different dataset without prior knowledge of the individuals' spindle amplitudes can be problematic [40]. Additionally, these fixed threshold-techniques do not take into account the spindle shape [40]. With adaptive thresholding, spindle amplitude variability between individuals has been taken into account [40]. However, the problem of excluding the spindle shape still remains [40].

Time-frequency analysis is a category of techniques in which both temporal and spectral properties of the signal are taken into account simultaneously [40]. This will

lead to optimized time-frequency resolution [40]. In this category, wavelet transform analysis is typically preferred [40]. In wavelet analysis, an appropriate mother wavelet is chosen, in the case of sleep spindles it is usually the Morlet wavelet (Figure 5) [40]. It has the desired spindle shape and thus it is often used [40]. Furthermore, wavelet analysis is applicable to non-stationary signals and thus is considered as a good choice for EEG signal analysis [40].

The newer methods include the use of machine learning in the detection of sleep spindles [40]. There are two different ways machine learning can be applied to spindle detection [40]. The algorithm can either learn the spindle characteristics through supervised learning from datasets where the spindles have been detected previously or the algorithm can be trained through unsupervised learning, where the machine can start detecting the spindles without any pre-existing information about the spindle waveform [40]. The supervised learning is more commonly used method, however, it is dependent on the quality of the datasets used in the teaching process [40]. If the the quality of the teaching dataset is poor, it will result in poor algorithm as well [40].

3.2 Slow wave oscillation

The terms used when describing slow wave sleep (SWS) can be confusing since the definitions for the terms tend to vary across different studies [52]. Genzel et al. noted that in human studies SWS refers to sleep stage N3 while in animal studies SWS refers to all NREM stages [52]. Therefore, in this thesis, the term SWS will be used to refer to N3 sleep stage. Following the definitions given by Leger et al., slow oscillation (SO) is an "oscillation visible in the local field potential (LFP) or EEG between 0.5 and 4.5 Hz" [53]. Furthermore, they define slow wave activity (SWA) as a "signal obtained after filtering in the low frequency range followed by a threshold to detect large fluctuation in the LFP/EEG during sleep" [53]. However, in the AASM manual SWA is defined as a signal with frequencies between 0.5–2 Hz [6].

The waveform of an SO is characterized by an upstate with positive voltage amplitude and a downstate with negative voltage amplitude [54]. During upstates, also known as depolarized states, local cortical neurons synchronously depolarize, and during downstates, or hyperpolarized states, local cortical neurons hyperpolarize [54]. According to the AASM, the peak-to-peak amplitude between the upstate and downstate of the SO must be >75 µV in the frontal derivations [6].

The origin of the SOs has not been fully determined. However, the cortex has been found to play a role in the generation of slow oscillations [55, 56]. In fact, Murphy et al. found that even disconnected cortical slabs still generate SOs [56]. Furthermore, a source modelling study has shown that the origin points of the slow waves center around the lateral sulci and then propagate into insular, parietal, temporal, and frontal cortices [55]. However, even though SOs have been shown to originate from several areas in the brain, studies have found that the SOs originate more frequently in anterior areas and propagate in anterior-posterior direction as traveling waves [55, 57]. Nevertheless, despite concluding that the SOs originate from the cortex, some subcortical structures have been hypothesised to contribute to the SO as well [54].

These subcortical structures include thalamus, basal forebrain, and brainstem nuclei [54]. There especially is an interest to find out whether the thalamus has an impact on, for example, the initiation, persistance, and termination of SO upstates [54].

The amount of SOs has been found to increase as the sleep progresses from wakefulness and light sleep to deep sleep [57]. Thus according to the AASM, if slow wave activity is detected in $\geq 20\%$ of the sleep stage epoch in question, that epoch should be scored as N3 sleep [6]. As with sleep in general, age has a big impact on the amount of SWS for humans. The amount of N3 has been found to decrease with increasing age [58]. Furthermore, N3 has been found to be more fragmented with older subjects compared to younger subjects [58].

Studies have found a link between disrupted N3 and Alzheimer's disease [59]. Additionally, a decrease in SWA has been found in patients with mild cognitive impairment [59]. Therefore, it has been suggested that reduced SWA during NREM sleep can be a biomarker for patients with Alzheimer's disease [59]. Furthermore, there is an interest to study whether it would be possible to restore SWA during NREM sleep in patients with Alzheimer's disease [59]. This could be done with transcranial direct current stimulation (tDCS) or transcranial magnetic stimulation (TMS) [59]. Both methodologies have resulted in an increase in SWA and improvement in memory tasks in human subjects [59].

3.3 Time synchronization of sleep spindles and slow wave oscillation

In addition to sleep spindles and SOs individually, their time synchronization and the effects of the time synchronization has been studied. In these studies, their coupling has been linked to brain plasticity and memory consolidation [17, 25, 40]. Furthermore, even though sleep spindles have been linked to memory consolidation on their own, cortical pyramidal cell activations by coupled SOs and sleep spindles have been found to be more powerful than the activation by just spindles alone [40].

Several factors have been linked to the location of the sleep spindles regarding the SO phase. These factors include the topographical location of the sleep spindles, the age of the subject, and whether the spindles are fast or slow. For example, Andrillon et al. found an increased number of spindles 0–500 ms after a negative slow wave peak [23]. They also noted that fast centroparietal spindles were more likely located in the upstates of a SO compared to frontal slow spindles [23]. Andrillon et al. also found that when detecting spindles in several parts of the brain, fast centroparietal spindles often appeared before slow frontal spindles [23]. These results were supported by Mölle et al. who found that fast spindles were often located at the up-state of the SO whereas slow spindles often occurred in the transition phase from the up-state to the down-state of the SO [24]. Muehlroth et al. found that with older subjects, the fast spindles did not occur at the SO peak, as is often the case in younger subjects [25]. However, older subjects were observed to have an increase in the slow spindle power at the end of the SO up-state [25].

Increased slow spindle occurrence at the end of the SO up-state was found to result in worse memory consolidation in younger subjects while fast spindle and SO coupling resulted in improved memory consolidation in both younger and older subjects [25]. Furthermore, Mölle et al. concluded that even though time synchronization of spindles and slow waves was present in subjects without prior learning, but the results were enhanced in subjects who did do a memory task prior sleeping [24]. Moreover, the coupling of sleep spindles and SOs has been found to decrease in older compared to younger subjects [17]. Enhancing the SWS without affecting the number of sleep spindles has not been found to enhance memory consolidation [60]. However, pharmacologically increasing sleep spindle and SO coupling has been found to result in improved verbal memory [61]..

The time synchronization between sleep spindles and slow wave oscillations has been studied using several different methods. These methods have included correlation histograms [16, 24], complex demodulation [26], power spectra [17], spectrograms [17], Hilbert transform [61], and modulation index [61], among others. They are based on filtering the signal in sleep spindle frequency, after which either thresholding or envelope power estimation often takes place.

4 Time-frequency analysis of non-stationary signals

This section focuses on the mathematical description of the signal analysis methods in the data analysis part of this thesis. These methods included empirical mode decomposition, the continuous wavelet transform, the Hilbert transform, and complex demodulation.

4.1 Empirical mode decomposition

Empirical mode decomposition (EMD) is a nonlinear data analysis method rivaling with Fourier spectral analysis [62]. Fourier transform is widely used in signal analysis and it has become the standard due to its less restrictive conditions compared to most data analysis techniques [62]. The restrictive conditions in Fourier analysis only include assumptions for linearity and stationarity [62]. Furthermore, in the cases where these assumptions are not fulfilled, Fourier transform is still useful if proper approximations are used on the data [62]. However, when using Fourier transform in cases where linearity and stationarity approximations are not valid, the results will have misleading harmonic components [62]. These harmonic components will cause energy spreading, leading to biased energy-frequency distribution [62]. This can issue a challenge when waveforms with certain frequency need to be detected, as the Fourier transform cannot distinguish instantaneous frequencies [62]. Therefore, other non-stationary data analysis techniques, such as EMD, are needed to extract the temporal frequency information in a time-series [62].

EMD is a method designed to decompose nonlinear and non-stationary signals [62]. In EMD, the idea is to decompose the signal into separate intrinsic oscillatory modes called intrinsic mode functions (IMFs) [62]. These IMFs are oscillatory signals, consisting of equal number of extremas and zero-crossings [62]. The decomposition is performed empirically, i.e., it is based on the time scales in the data [62]. The time scales were defined by Huang et al. as the time lapse between successive extrema [62]. Choosing the time scales as aforementioned leads to better resolution of oscillatory modes than if the time scales were defined as time lapses between successive zero crossings [62]. This choice also allows EMD implementation to data with non-zero mean [62].

The IMFs can be extracted from the signal with a process of shifting [62]. In shifting two envelopes are drawn for the maximum and minimum values of the signal, for example with cubic splines [62]. After this, all the data should be located between the maximum and minimum envelope [62]. Furthermore, the mean of the two envelopes is calculated and this mean is then subtracted from the original data [62]. If the resulting signal is a zero-mean signal, the first IMF has been created [63]. If the resulting signal does not have a zero mean, the shifting process is repeated on the subtracted signal of two previous consecutive iterations until the zero-mean condition is fulfilled, in which case the first IMF has been created [63].

The second IMF can be extracted in the same manner, implementing the shifting process on a residual signal obtained by subtracting the first IMF from the original signal [63]. This process can be continued until the residual signal is a monotonic function or a signal with one maximum and one minimum (Figure 3) [63].

The aim of the shifting process is to remove any riding waves, which can be described as, for example, a maximum that does not cross the zero line between two consecutive minimas [62]. This is important for making the instantaneous frequency meaningful, i.e., in order to the Fourier transform of the real part of the signal to have only positive frequencies [62]. If any negative frequencies are present, which is the case in riding or asymmetrical waves, the instantaneous frequency is not defined [62]. Also with shifting, the aim is to produce more symmetric waveforms which is important for cases where the neighbouring wave amplitudes differ considerably [62]. This smoothing of uneven amplitudes may come at a cost if the shifting process is continued for too long, causing some physically significant waveforms to disappear [62]. Therefore, it is important to have some stopping criteria for the shifting process in place [62].

EMD can be useful in signal event detection due to the extracted IMFs being symmetric in respect to the local zero mean, and having an equal number of zero crossings and extrema [62]. With these characteristics it is possible to utilize the concept of instantaneous frequency to localize an event from the signal [62].

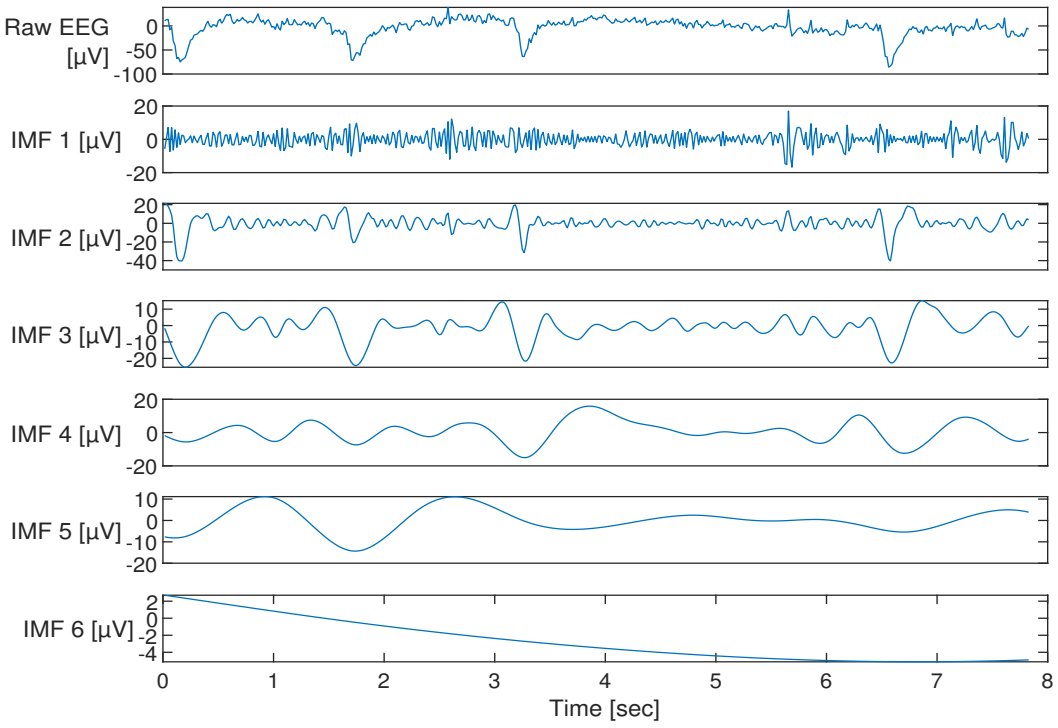

Figure 3: The original electroencephalogram (raw EEG) and the first six of its intrinsic mode functions (IMFs) obtained through empirical mode decomposition.

4.2 Continuous wavelet transform

The continuous wavelet transform (CWT) is a popular tool in time-frequency analysis of non-stationary signals [64]. The main reason for this is the accurate time-frequency localization of the CWT [64]. With other methods, such as the Fourier transform, even though the information of the frequency content of the signal is obtained, the temporal locations of the frequency features are not given [64]. This can be addressed with a windowed Fourier transform, also known as the short-time Fourier transform (STFT) [64]. However, choosing the window function can be challenging if there are signal features of different scales to be recognized [64]. Furthermore, for the STFT, the signal is required to be piece-wise stationary, and additionally, preserving sufficient frequency and time resolution simultaneously can be challenging [63]. Thus, in these cases, the CWT can be a useful option due to its capability to change according to the analyzed frequency content [64].

The CWT is defined as

$$\begin{aligned} Wf(u,\lambda) &= \int_{-\infty}^{\infty}\int_{-\infty}^{\infty} f(t)\psi_{u,\lambda}(t)dt, \quad \lambda > 0 \\ &= \int_{-\infty}^{\infty}\int_{-\infty}^{\infty} f(t)\frac{1}{\sqrt{\lambda}}\psi\left(\frac{t-u}{\lambda}\right)dt, \end{aligned} \tag{1}$$

where t denotes time, $f(t)$ is the signal for which the wavelet transform is calculated and $\psi_{u,\lambda}(t)$ denotes a wavelet, also referred to as the mother wavelet, with a scaling parameter λ and a temporal location parameter u [65]. The mother wavelet must satisfy an admissibility condition

$$C_\psi = 2\pi \int_{-\infty}^{\infty} \frac{|\hat{\psi}(\omega)|^2}{|\omega|} d\omega < \infty, \tag{2}$$

where C_ψ is the admissibility constant, $\hat{\psi}$ is the Fourier transform of the wavelet function ψ and ω is frequency [66]. Condition 2 holds for wavelet functions if $\psi \in L^2(\mathbb{R})$. However, if $\psi \in L^1(\mathbb{R})$ and therefore $\hat{\psi}$ is continuous, (2) is still true if the condition $\hat{\psi}(0) = 0$, i.e., $\int \psi(x)dx = 0$ holds [66]. If the chosen wavelet is of complex form, $\psi_{u,\lambda}(t)$ is replaced with the complex conjugate of the wavelet $\overline{\psi}_{u,\lambda}(t)$ [64]. Furthermore, to achieve temporal localization, the mother wavelet must have compact support or decay fast [64].

Depending on the application, the wavelet can be modified with the choice of λ, as the temporal width of the wavelet varies directly proportional to λ, and the width of the wavelet's frequency band varies inversely proportional to λ. If $\lambda > 1$, the wavelet is stretched along the temporal axis and contracted along the frequency axis, and vice versa, if $\lambda < 1$. This can be illustrated with Heisenberg boxes in time-frequency plane (Figure 4). [65] Additionally, the choice of u will result in a directly proportional shift in the temporal location of the wavelet $\psi_{u,\lambda}(t)$ [64].

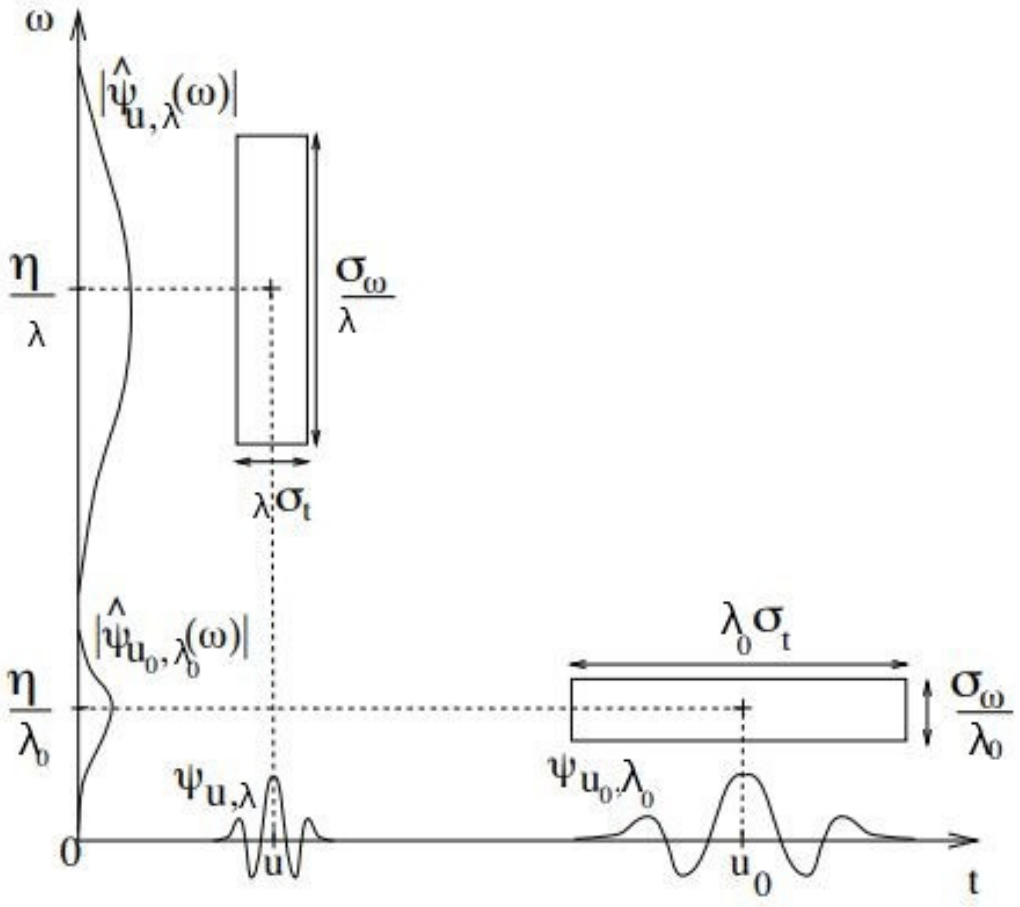

Figure 4: Two wavelets $\psi_{u,\lambda}$ and ψ_{u_0,λ_0}, presented as Heisenberg boxes in time-frequency (t,ω)-plane. σ_t represents the time width and σ_ω represents the frequency height of the Heisenberg box. $|\hat{\psi}_{u,\lambda}(\omega)|$ and $|\hat{\psi}_{u_0,\lambda_0}(\omega)|$ represent the energy spreading of the two wavelets. The boxes are located at time points u_0 and u and they are dilated or contracted according to the scale parameters λ_0 and λ. The scale parameter also determines the positive frequency interval, centered around η/λ or η/λ_0. Picture modified from [65].

As the purpose of the study was to detect patterns such as sleep spindles, Morlet wavelet was chosen as the mother wavelet due to its suitable form. The Morlet wavelet is defined as

$$\psi(t) = \pi^{-1/4}(e^{-i\omega_0 t} - e^{-\omega_0^2/2})e^{-t^2/2}, \tag{3}$$

where i is the imaginary unit and ω_0 is the center frequency [67]. Furthermore, if $\omega_0 \geq 5$, the equation can be approximated as

$$\psi(t) = \pi^{-1/4}e^{-i\omega_0 t}e^{-t^2/2}, \tag{4}$$

since the term $e^{-\omega_0^2/2}$ in (3) becomes negligible [64]. However, the Fourier transform of (4) is

$$\hat{\psi}(\omega) = \sqrt{2}\pi^{1/4}e^{-1/2(\omega-\omega_0)^2} \tag{5}$$

and thus, the admissibility condition

$$\hat{\psi}(0) = \sqrt{2}\pi^{1/4}e^{(-\omega_0)^2/2} \neq 0 \tag{6}$$

is not fulfilled [67]. Nevertheless, for $\omega_0 \geq 5$, the Fourier transform of (4) becomes

$$\hat{\psi}(\omega) \approx 0, \quad \omega \leq 0, \tag{7}$$

thus satisfying the admissibility condition [64, 67]. From (4), a Gaussian function $e^{-t^2/2}$ can be observed to modulate the harmonic oscillating function $e^{-i\omega_0 t}$ [20]. Thus, the shape of the Morlet wavelet is similar to a sleep spindle (Figure 5). Additionally, it is a complex function, which makes the extraction of the phase and the amplitude feasible [64]. Furthermore, the wavelet energy can be calculated as

$$E(u, \lambda) = |W(u, \lambda)|^2. \tag{8}$$

The wavelet energy describes the distribution of spectral power of the signal [20]. It can be used to detect the sleep spindles by setting a threshold at which a waveform is considered to be similar enough to the mother wavelet that it can be considered a sleep spindle [20].

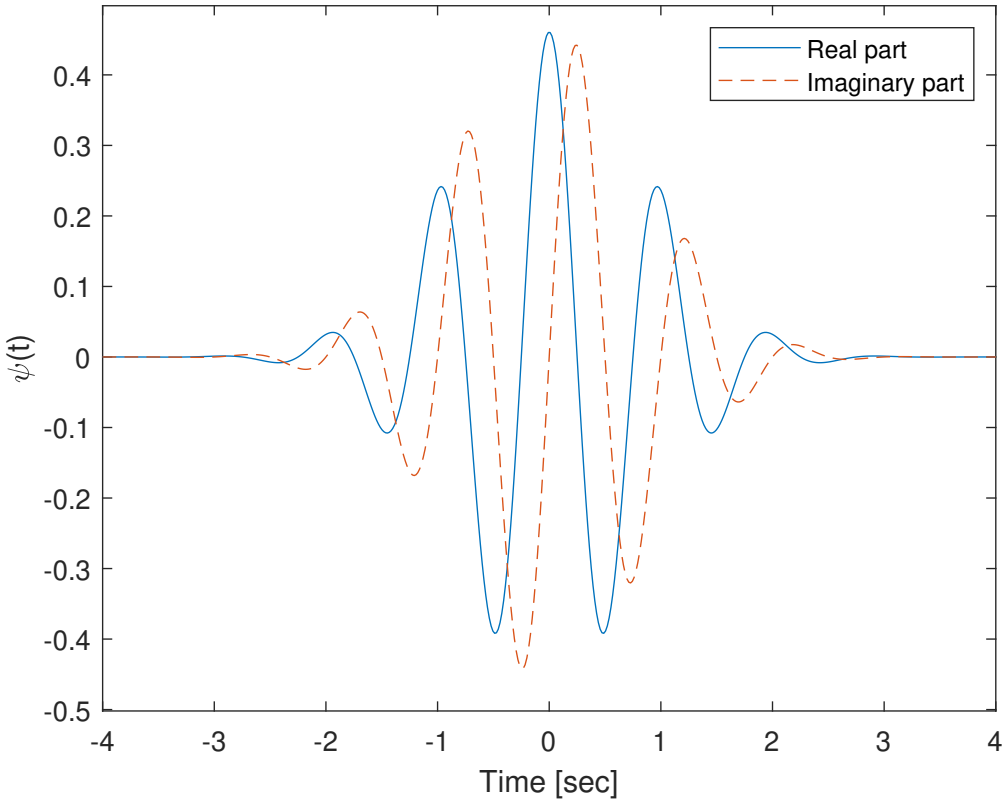

Figure 5: The Morlet wavelet $\psi(t)$. The solid line represents the real part and the dotted line represents the imaginary part of the wavelet.

4.3 Hilbert transform

The Hilbert transform (HT) is a signal analysis tool which transforms a real signal $x(t)$ into a complex valued signal $z(t)$,

$$z(t) = x(t) + iH(t), \tag{9}$$

where $H(t)$ is the HT of a real signal $x(t)$, i is the imaginary unit $i = \sqrt{-1}$ and t denotes time. In other words, the transform produces a complex component $H(x(t))$ for the real signal $x(t)$ and as a result an analytical signal $z(t)$ is obtained. Obtaining an analytical signal allows the extraction of instantaneous phase and amplitude of the signal $x(t)$. [68] The instantaneous phase $\phi(t)$ can be calculated as

$$\phi(t) = \arctan\left(\frac{\mathrm{Im}(H(t))}{\mathrm{Re}(H(t))}\right), \tag{10}$$

and instantaneous amplitude $a(t)$ as

$$a(t) = \sqrt{\mathrm{Re}(H(t)) + \mathrm{Im}(H(t))}. \tag{11}$$

Furthermore, the HT is defined as

$$H(t) = \frac{1}{\pi}\mathrm{P}\int_{-\infty}^{\infty}\frac{x(\tau)}{t-\tau}d\tau, \tag{12}$$

where τ is the integration variable and P represents Cauchy's principal value [62]. The HT is a convolution between the original real signal and the impulse response (12) [69].

The HT extends a two-dimensional real signal into a three-dimensional complex signal. In practice this means that after the HT, the difference between the original real signal $x(t)$ and the new complex valued signal can be seen in the frequency content. The positive frequency components of the real signal $z(t)$ are equal to the positive frequency components of the real signal $x(t)$ but shifted by $-\pi/2$ in phase. Similarly to the negative frequency components but this time the phase shift is $\pi/2$. [70]

The usefulness of the Hilbert transform lies in its ability to extract the instantaneous envelope and phase of a signal waveform [70]. Due to its complex form, the extracted envelope is more accurate than in other methods such as amplitude demodulation, might produce [70]. From the instantaneous phase it is possible to calculate the instantaneous frequency of the signal which is crucial in applications studying the time synchronization of signal waveforms [70]. Furthermore, the HT is also popular due to its simplicity, as there is no need for domain changes [69]. If the HT is performed on a signal in time domain, the resulting signal will be in time domain as well [69]. As the same applies in frequency domain, the computational demand of the technique is little compared to techniques that require domain changes [69].

4.4 Complex demodulation

Complex demodulation is a technique in the analysis of modulated signals [71]. The idea behind complex demodulation is to acquire a complex representation of an analytic signal [72]. Therefore, after acquiring the complex form of the real signal by complex demodulation, the envelope and phase functions can be extracted. The envelope function describes the energy of the signal, and therefore, any maximum peaks observed in the envelope function can be utilized to localize any transient waves [71]. Additionally, the phase function and more importantly, the first derivative of this phase function, describes the instantaneous frequency of the signal.

Complex demodulation can be performed in the time domain as follows: the analytic signal $x(t)$ can be modelled as

$$x(t) = A(t)\cos(f_0(t) + h(t)), \tag{13}$$

where t denotes time, f_0 is the center frequency, $A(t)$ is the amplitude function and $h(t)$ denotes the phase function [73]. Furthermore, by using Euler's equation, (13) can be expressed as

$$x(t) = A(t)(e^{i(f_0 t + h(t))} + e^{i(-f_0 t + h(t))})/2. \tag{14}$$

Now, after expressing the analytic signal in a polar form, the signal equation is multiplied with exponential function $e^{-if_0 t}$. This will result in the spectrum of the analytic signal $x(t)$ to be shifted towards the origin by f_0 (Figure 6)[73]. Thus

$$\begin{aligned} z(t) &= x(t)(2e^{-if_0 t}) \\ &= A(t)(e^{ih(t)} + e^{-i(2f_0 t + h(t))}). \end{aligned} \tag{15}$$

After shifting the spectrum of the analytic signal, the signal $z(t)$ is lowpass filtered to obtain the spectra of the signal components that are of interest (Figure 6). The resulting signal $y(t)$ is of form

$$y(t) = A(t)e^{ih(t)}, \tag{16}$$

which is also the complex envelope of the analytic signal $x(t)$. Furthermore, the envelope function is

$$A(t) = |y(t)| \tag{17}$$

and the phase function is of form

$$g(t) = f_0 t + \tan^{-1}\left(\frac{\mathrm{Im}(y(t))}{\mathrm{Re}(y(t))}\right). \tag{18}$$

To be able to extract the envelope and phase functions appropriately, the signal is required to be a bandpass type [73]. Therefore, a preprocessing step might be needed and hence, the total process of complex demodulation includes two filtering steps [71]. This results in two convolution integrals to be performed in time domain, which leads to increased computation time [71]. To address this issue, complex demodulation has been suggested to be performed in frequency domain instead of time domain, thus decreasing the amount of convolution integrals needed in the process [71]. However, despite the possible computational demands, Ktonas et al. have pointed out that complex demodulation is the most effective and flexible technique to implement in demodulation applications [71].

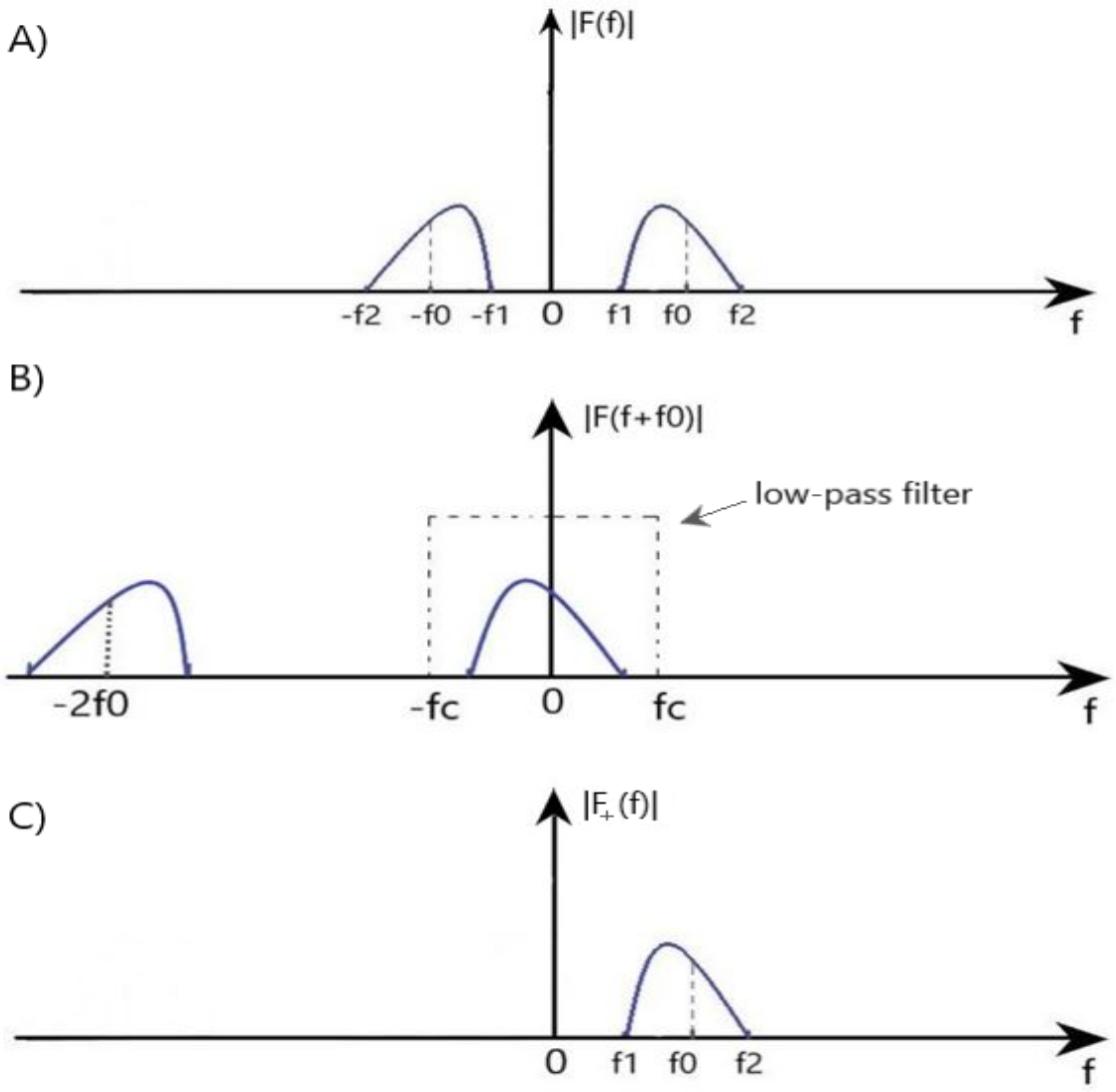

Figure 6: Complex demodulation performed in frequency domain. *F(f)* denotes the frequency spectrum, f is the frequency and $F_+(f)$ is the positive frequency spectrum. Furthermore, f_0 is the central frequency of the frequency spectrum, f_1 is the first frequency value of the spectrum and f_2 is the last frequency value of the spectrum. A) Initial frequency spectrum of a real signal. B) Frequency spectrum is shifted by frequency f_0. C) After lowpass filtering, only the desired frequencies are left.

5 Aims and hypotheses

The aim of this Master's thesis was to investigate the time synchronization of sleep spindles and slow wave oscillation in nocturnal EEG signals using complex demodulation and the Hilbert transform. The aim was to compare the obtained time synchronization results between these two methods and to investigate whether the different methods affect the perceived position of the sleep spindles in reference to the slow waves. Additionally, the aim was to investigate two different approaches, first by detecting slow waves and performing a time synchronization analysis and secondly, detecting spindles from the slow waves, and then performing the time synchronization analysis. The aim was to compare these two approaches to study if any major differences between these approaches were observed.

We hypothesized that the time synchronization between the sleep spindles and slow waves can be found using both methods and that similarly to previous literature the sleep spindles would be located in the positive peak of the slow wave. Furthermore, we hypothesized the time synchronization results obtained with the different methods and approaches mainly support each other, possibly having only minor discrepancies.

6 Methods

In this section, the methods of the thesis study are explained. This section describes the used dataset (Section 6.1), and the detection of the slow waves (Section 6.2) and sleep spindles (Section 6.3). Additionally, the the time synchronization and coupling analyses between sleep spindles and slow waves are described (Section 6.4). All analyses were carried out using MATLAB R2019b (MathWorks, 174 Natick, Massachusetts, USA).

6.1 Data

The data used in this study was a collection of EEG signals from diagnostic type I PSGs. The PSGs were recorded in Australia at the Sleep Disorders Center of Princess Alexandra Hospital (Brisbane, Australia) from 899 patients with suspected obstructive sleep apnea. The data was collected in 2015–2017 with an acquisition system Compumedics Grael (Compumedics, Abbotsford, Australia) and the collection was approved by the Institutional Human Research Ethics Committee of the Princess Alexandra Hospital (HREC/16/QPAH/021 and LNR/2019/QMS/54313).

The maximum power spectra of slow sleep spindles and SO frequencies have been found in the fronto-central derivations of EEG [24]. Additionally, the maximum power spectrum for fast sleep spindle frequencies has been found in the centro-parietal derivations of EEG [24]. Therefore, the chosen EEG signals for this study were from the channel C4-M1, i.e., a central channel of EEG. The signal was recorded with 1024 Hz frequency and for signal analysis purposes, the signal was downsampled to 64 Hz after lowpass-filtering in frequency range 1–128 Hz, according to the Nyquist theorem to avoid any aliasing during downsampling. In addition to the EEG-signals, every patient had manually scored sleep stages available. Furthermore, since the epochs scored as N3 include both sleep spindles as well as slow wave activity [37], only these were chosen to be analyzed.

6.2 Slow wave detection

The amplitude of normal human EEG is in the range of 20–100 µV [11]. Therefore any N3 epoch containing EEG amplitude higher than 250 µV was excluded. After the artefact exclusion, the N3 epochs of interest were bandpass filtered in the range of 0.5–2 Hz. The bandpass filter was a Finite Impulse Response (FIR) filter with order of 60 and sampling frequency of $f_s = 64$ Hz. From the filtered EEG, slow waves were detected using a similar approach as Dang-Vu et.al [74]: the slow wave negative peak amplitude should exceed 80 µV, and the combined amplitude of the negative and the positive slow wave peaks should be higher than 140 µV. In addition to the amplitude criteria, the duration of the negative slow wave peak should be in the range of 300–1500 ms and the duration of the positive slow wave peak should be <1000 ms (Figure 7). If a slow wave fulfilling the criteria was detected, a segment of raw EEG with duration of 5 seconds was extracted. The segments fulfilling these criteria were position-locked, i.e., the negative slow wave peaks were placed 2.5 seconds from the

start of each segment.

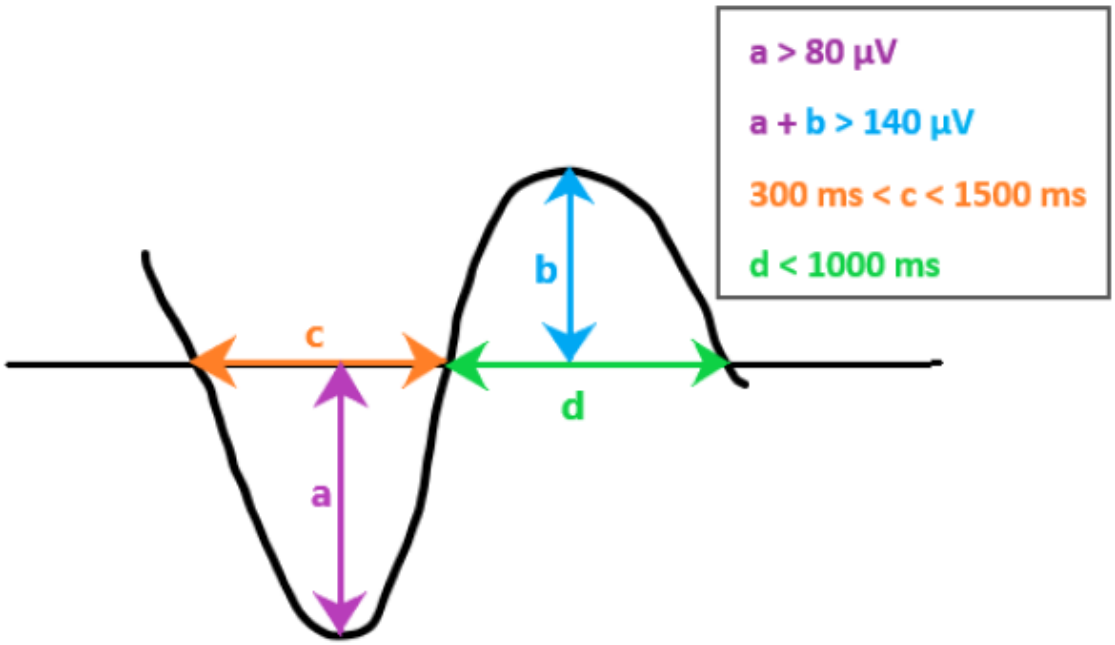

Figure 7: Slow wave detection criteria.

6.3 Sleep spindle detection

Spindle detection was performed with a combination of EMD and wavelet transform by using a method previously described by Grubov et al. [20]. EMD was performed to the 5 seconds long segments of slow wave-locked signals and thus, the IMFs were obtained. For the spindle detection, the first IMF was chosen, since it contains the frequencies of sleep spindles [20]. After obtaining the first IMF of the signal, the CWT was performed using (1) to detect sleep spindles from the signal using the Morlet wavelet as the mother wavelet due to its similar shape to a sleep spindle. The wavelet coefficients and u (1) were obtained from the the CWT, out of which the coefficients corresponding to spindle frequencies (11–16 Hz) were chosen. Furthermore, the wavelet energies were computed using (8). As several wavelet coefficients were obtained due to the use of dilated and contracted variations of the mother wavelet, a mean of the wavelet energies was calculated within the frequency band. Additionally, to avoid short-time artifacts and the following pattern recognition errors, temporal mean wavelet energy was calculated using moving average.

From the mean wavelet energy spectrum, all the positive peaks were identified, as they corresponded to possible sleep spindles. Moreover, to choose the most probable sleep spindles out of all the peaks, a threshold was chosen. If the peak in the wavelet energy spectrum was higher than 70% of the mean value of the peaks, a possible spindle was detected (Figure 8). As spindles should range between 0.5–3 seconds in duration, wavelets with durations outside this range were discarded as not spindles.If

a spindle was not found in a slow-wave segment, that segment was excluded from the analyses. After detecting the spindles, 4-second-segments, ±2 seconds around the maximum amplitude points of the spindles were separated from the spindle filtered EEG. These segments were then position-locked to the maximum amplitude point of each spindle, determined from the first IMF of the EEG.

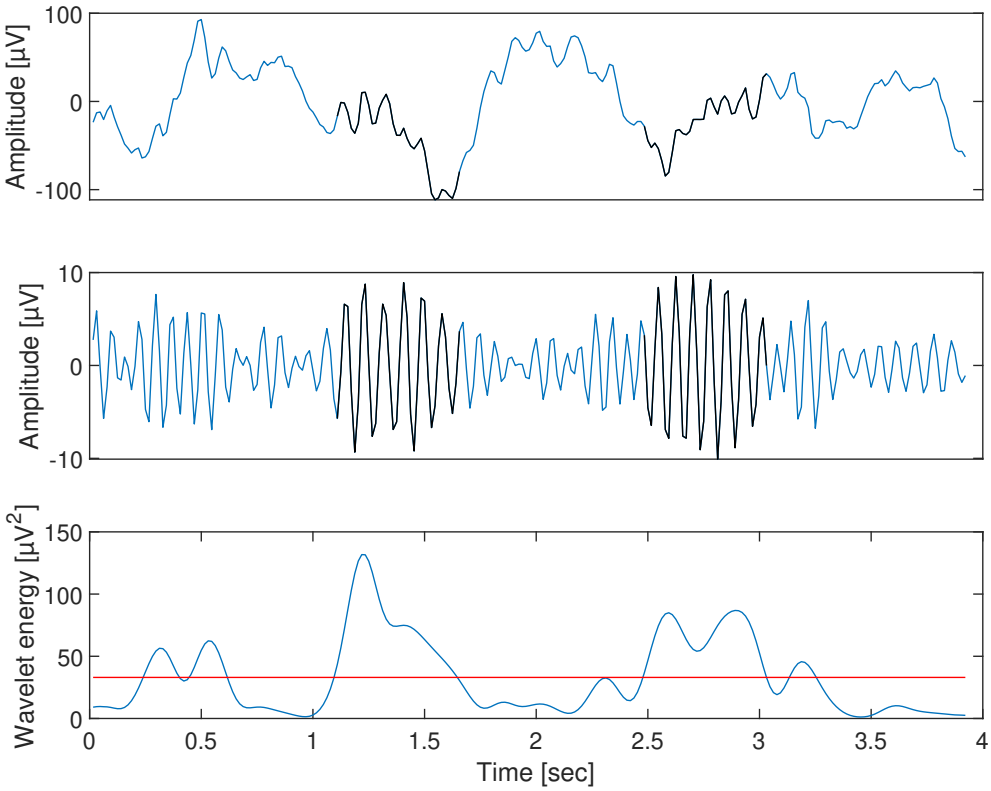

Figure 8: Spindle detection. First figure shows the raw electroencephalogram (EEG) signal, second figure shows the first intrinsic mode function (IMF) and the last figure shows the wavelet power spectrum. In addition in the wavelet power spectrum, there is a threshold presented in red, which is the 70% of the mean of the peak values. Even though several peaks surpassed this threshold, they might not have been desired length and thus were excluded from spindle detection. The detected spindles are marked as black in the raw EEG signal as well as in the IMF signal.

6.4 Sleep spindle and slow wave coupling

As a result of the slow wave and spindle detection, two separate datasets were formed: one including the EEG-segments that were position-locked according to the slow waves, and another one including essentially the same EEG-segments, but position-locked according to the corresponding spindles. Hence the two data-sets were equal-sized, as one slow wave in the first dataset was always related to one spindle in the second dataset. The coupling of these spindles and slow wave oscillations was studied by using the HT as well as complex demodulation. The analyses were done using two approaches, i.e., on two datasets; first on the dataset including the position-locked sleep spindles and then on the dataset including the position-locked slow waves. The the HT and complex demodulation were applied to both datasets to study the time synchronization.

The HT was calculated for each signal from both spindle-locked and slow wave-locked datasets using (12). For the HT, EEG segments during the slow wave- and spindle-locked segments were filtered with FIR band-pass filters (f_s = 64, filter order = 60) to obtain the slow wave oscillation in frequency range of 0.5–2 Hz and spindle oscillation in frequency range of 11–16 Hz. Before further analyzing, the filtered slow wave segments were shortened from 5 seconds to approximately 2 seconds in length, while maintaining the position-locking. The extra length was cut from both ends of the signals to avoid any effects of the filtering on the HT. The HT was calculated for the filtered slow wave oscillation and the phase of the slow wave was obtained using (10).

Similarly, for the spindle-locked dataset, the segment lengths were shortened from 5 seconds to 2 seconds, to avoid filtering effects on the HT. With the HT, the amplitude of the filtered spindle oscillations were calculated using (11). Furthermore, mean spindle amplitude in each slow wave phase was calculated. The spindle amplitudes were then normalized with the mean of the mean amplitudes across all slow wave phases, i.e. the grand-mean. By normalizing the amplitudes with the grand-mean, it is possible then to compare the results with other studies, where the absolute values might differ greatly from our own results. Additionally, the maximum amplitudes, i.e., the maximum amplitude of each spindle, and their location were calculated.

For the same position-locked signal segments, complex demodulation was computed. The signals were band-pass filtered with the same filter as previously to obtain the signal in spindle frequencies 11–16 Hz. The envelopes of the spindle-filtered signals were computed using (17) (Figures 9a and 9c) and the powers of the envelope were obtained by calculating the square of the envelope amplitudes (Figures 9b and 9d).

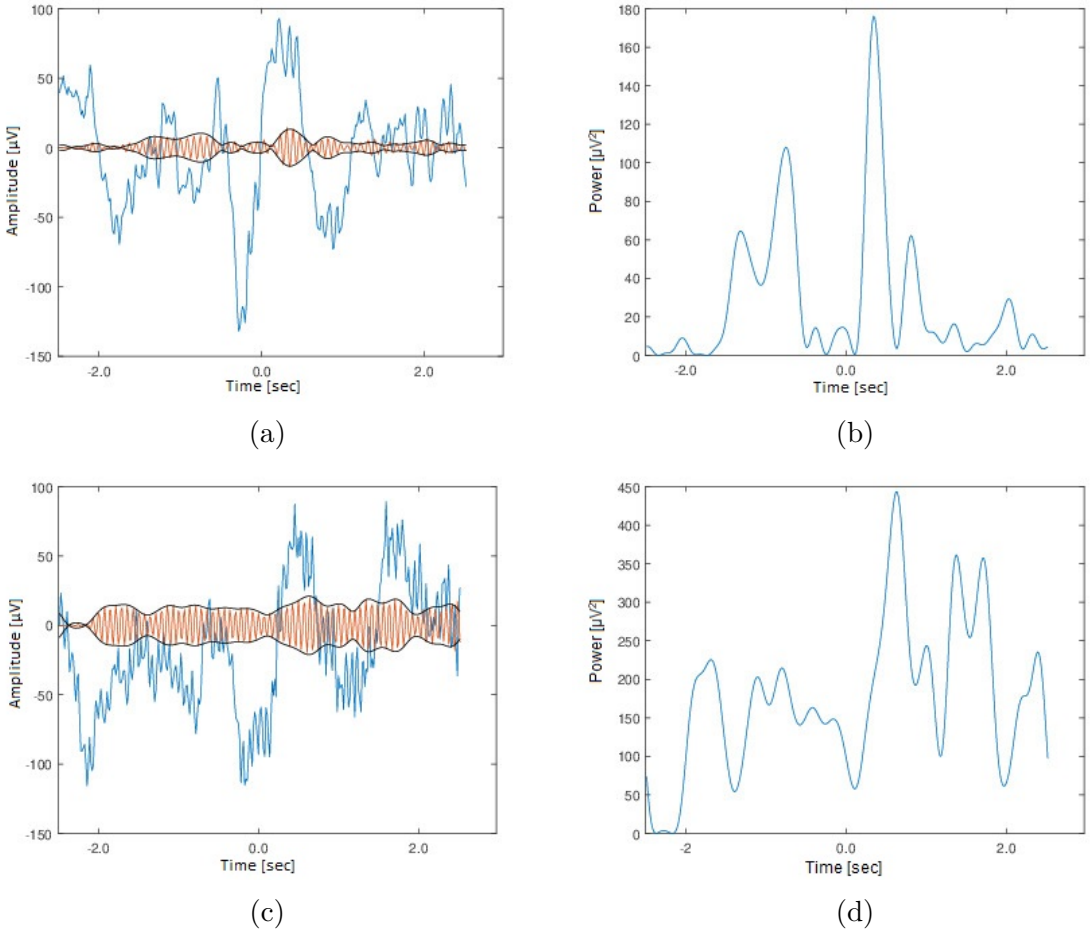

Figure 9: Examples of complex demodulation. In a) and c) the raw position-locked slow wave signal is presented in blue and the signal filtered in spindle frequencies in orange. Furthermore, the envelopes obtained through complex demodulation are presented in black. In b) and d) the power of the envelopes in a) and c), respectively, are presented.

7 Results

In this section, the results of the thesis are presented. First, the results of the HT are presented in section 7.1. The results for slow wave-locked segments and spindle-locked segments are presented in the sections 7.1.1 and 7.1.2, respectively. Furthermore, results of the complex demodulation are presented in section 7.2. The results for slow wave-locked segments and spindle-locked segments are presented in the sections 7.2.1 and 7.2.2, respectively.

7.1 Hilbert transform

7.1.1 Slow wave-locked segments

Mean instantaneous spindle amplitudes were the lowest between the slow wave phases $\pi/2$ and π, which corresponds to the decreasing slope after the slow wave peak, and the highest between the slow wave phases $3\pi/2$ and 0 (Figure 10a). This translates to the increasing slope of the slow wave before the positive peak.

Higher maximum spindle amplitudes were observed around the positive peak of the slow wave, i.e., between phases $3\pi/2$ and $\pi/2$ than around the negative peak, i.e., between phases $\pi/2$ and $3\pi/2$ (Figure 10b). These phases $3\pi/2$ and $\pi/2$ correspond the middle points of the increasing and decreasing slopes of the slow wave.

7.1.2 Spindle-locked segments

Mean instantaneous spindle amplitudes were the lowest between the slow wave phases $\pi/2$ and π, corresponding to the decreasing slope of the slow wave. The highest amplitudes were observed between the slow wave phases $3\pi/2$ and $\pi/2$ (Figure 10c). This translates to the middle of the increasing slope and the positive peak of the slow wave.

Higher maximum spindle amplitudes were observed between the slow wave phases $3\pi/2$ and 0 (Figure 10d), which translates to the increasing slope of the slow wave before the positive peak. Even though these were the highest, other peaks between the phases 0 and $\pi/2$ were close in value as well, which would correspond to the decreasing slope, right after the positive peak of the slow wave.

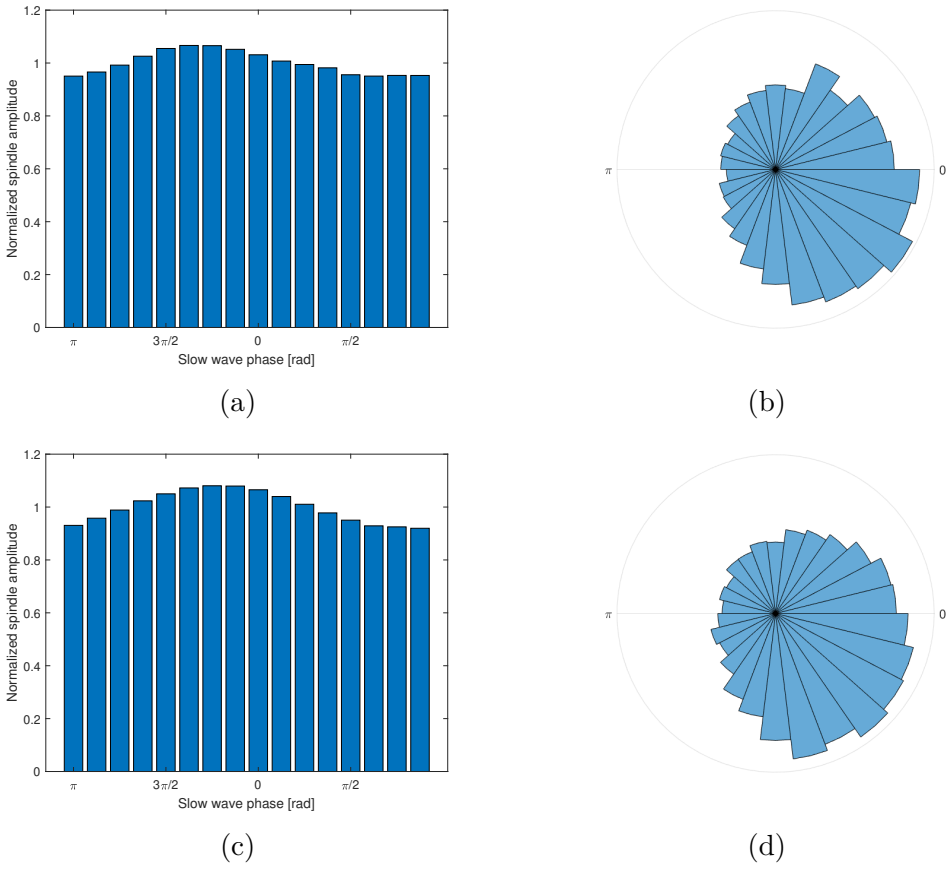

Figure 10: The mean instantaneous spindle amplitudes are presented as a function of the mean slow wave phase during a) slow wave-locked segments and c) spindle-locked segments. The amplitudes were normalized with the grand-mean. The maximum amplitudes of the spindles in the corresponding slow wave phases are shown during b) the slow wave-locked segments and d) spindle-locked segments.

7.2 Complex demodulation

7.2.1 Slow wave-locked segments

From the mean power of the complex envelopes, five peaks were observed, indicating a possible spindle (Figure 11c). The first smaller spindle peak occurred in the beginning of the slow wave, i.e., already before the slope of the negative amplitude. The next peak was observed at the decreasing slope of the slow wave, before its negative peak. The third and the highest peak in the power envelope was observed in the increasing slope of the slow wave, before its positive peak. In addition, two similar but slightly smaller peaks closely followed the highest peak, effectively forming one wide spindle peak extending over the positive amplitude of the slow wave.

Additionally, the mean of the spindle-filtered segments was calculated (Figure 11a) to investigate whether the shape of the spindle could be observed and whether its location matched with the complex envelope power peaks. However, no clear spindle shape was observed from the result.

7.2.2 Spindle-locked segments

The results obtained through complex demodulation (Figure 11d), showed that after obtaining the mean power of the signal envelopes, two smaller peaks and one higher peak could be observed. The first peak was located at the decreasing slope of the slow wave, before the negative peak. The second and the highest peak in the complex envelope was located at the positive peak of the slow wave. However, the shape of the slow wave diminished by the third complex envelope peak, so no clearly distinguishable position in reference to the slow wave was observed. In addition from the mean spindle filtered signal, one spindle shape was observed and its maximum point was located after the positive peak of the slow wave (Figure 11b).

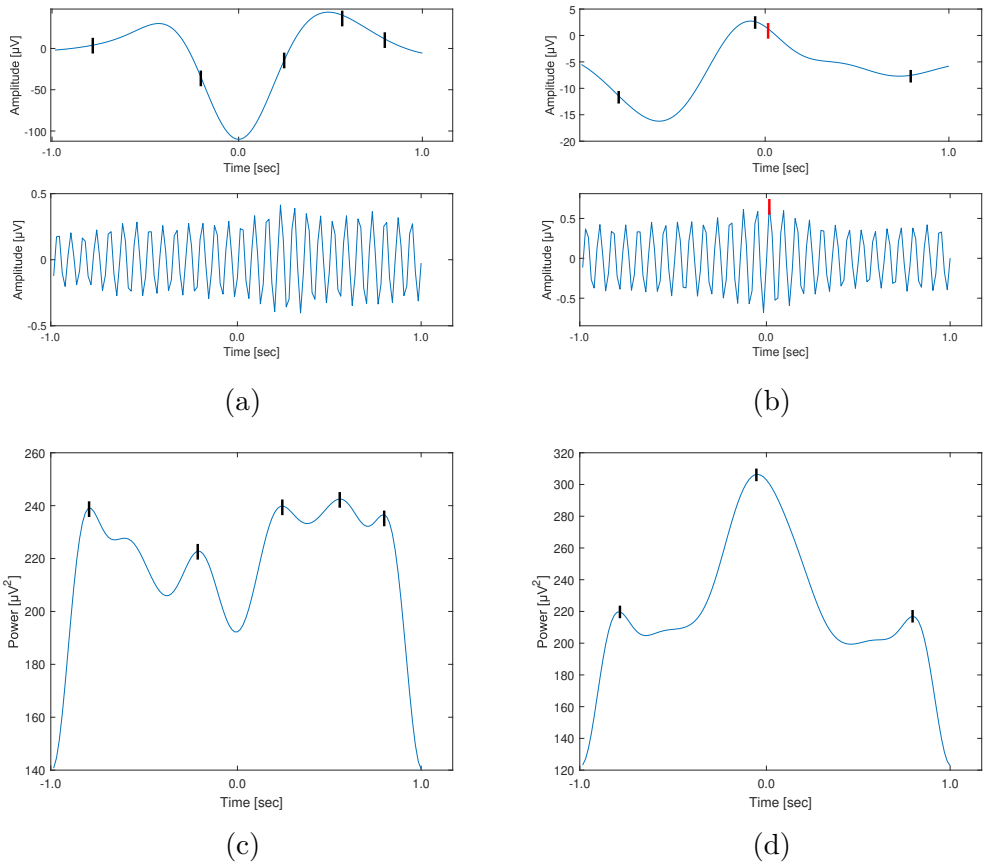

Figure 11: Means of differently decomposed electroencephalogram segments including the same spindles and slow waves, but position-locked according to the location of the a) and c) slow waves, and b) and d) spindles. Means of the slow wave filtered (0.5–2 Hz) signals are presented in the upper figures of a) and b). Lower figures of a) and b) show the mean of the spindle filtered (11–16 Hz) signals. In c) and d), the mean power of the complex envelopes are presented, calculated with complex demodulation. The black lines on figure mark the locations of the corresponding complex envelope peaks and the red lines present the location of the maximum points of the spindles, observed from the mean spindle-filtered signal.

8 Discussion

In this thesis we studied time synchronization of sleep spindles and slow wave oscillation in nocturnal EEG signals and the location of the sleep spindles in reference to the slow waves. First, slow waves and their related spindles were detected and separated from the signals. After that, two signal analysis methods (the HT and complex demodulation) were used to study their time synchronization. In addition, both of these analysis methods were implemented using two different approaches. In the first approach, the spindles were position-locked to obtain the location of the related slow waves, and in the second approach this was done the other way round. The results showed indications of time synchronization between sleep spindles and slow wave oscillation. In the spindle-locked dataset, the results showed strongest coupling between spindles and slow waves in the increasing slope and the positive peak of the slow wave. This notion was supported by the results from the HT. The results from complex demodulation supported the notion, that the spindles were observed at the positive peak of the slow wave. In the slow wave-locked dataset, similar results were obtained as the strongest coupling of sleep spindles and slow waves were observed in the increasing slope of the slow wave. These results were supported by both methodologies, complex demodulation and the HT.

Time synchronization between sleep spindles and slow waves has been reported in previous studies [24, 25, 26, 61]. Fast spindles have been reported to be coupled with the positive peak of the slow wave [24, 25, 26] and slow spindles have been observed to be coupled with the slow wave at the transition to the slow wave decreasing slope [24, 25, 26]. Furthermore, Yordanova et al. were able to distinguish that fast spindles would locate themselves either at the ascending slope of the slow wave, after the negative peak or right before the positive peak of the slow wave [26]. In this study, sleep spindles were not separated into fast or slow spindles. However, although separating fast and slow sleep spindles was outside the scope of this study, similar results were obtained.

From the spindle-locked results, the HT showed that the most spindles would be present right before the positive peak of the slow wave. Similar results were obtained for the slow wave-locked segments, where in the HT results, most spindles were observed closer to the middle point of the increasing slope of the slow wave, rather than the positive peak. The results from the complex demodulation for spindle-locked segments showed the highest spindle-related complex envelope peak at the positive peak of the slow wave. For slow wave-locked segments, complex demodulation showed the highest spindle-related complex envelope peak at the ascending slope of the slow wave. However, the peak of the complex envelope was quite wide, consisting of two additional smaller peaks. Thus, the peak continued from the ascending slope of the slow wave through the positive peak to the beginning of the descending slope of the slow wave.

Additionally, even though most spindles detected during N3 sleep stage have been considered to be slow spindles, fast spindles can also be observed in the central derivations [40]. Furthermore, Gibbs et al. have noted that slow spindles can be observed in the frontal derivations of EEG and fast spindles in the posterior derivations [46]. Therefore, considering the abovementioned as well as the previous literature [24, 25, 26], it is possible that the spindles detected the most in this study were fast spindles.

The results from the HT in the spindle-locked dataset showed that there was another point where a slightly higher amount of maximum spindle amplitudes were detected. This point was found between the phases 0 and $\pi/2$, which translates to the beginning of the decreasing slope of the slow wave. Correspondingly, complex envelope of the slow wave-locked signals showed a peak in the middle section of the decreasing slope of the slow wave. Similar results were obtained from the HT as well. These observations are supported by the study done by Yordanova et al., where they observed that slow spindles were coupled to the downstate of the slow wave [26]. Thus, it is possible that the peak observed at the descending slope of the slow wave in the present study is due to detection of slow spindles. The smaller height of the peak compared to the peak at the ascending slope could be explained by the fact that even though sleep stage N3 includes mainly slow sleep spindles [40], they are mostly detected from the frontal derivations of EEG [46].

The sleep spindles were detected by using a method introduced by Grubov et al. [20], where they were able to successfully detect sleep spindles by using a combination of EMD and the CWT. The mean spindle filtered signal of the spindle-locked segments showed one sleep spindle shape and the spindle had its maximum amplitude at the point 0.1 s. This point agreed with the 1st IMF-based maximum amplitude point, where the spindles were originally position-locked (at 0.0 s). Additionally, in the complex envelope of the spindle-locked segments, the most prominent peak was also observed approximately at the time point of 0.0 s, where the detected sleep spindles were time-locked. Thus, these results imply, that the complex demodulation was able to detect the same spindles as the spindle detection algorithm.

Even during the spindle-locked segments, the mean slow wave filtered signal revealed a slow wave shape, although it did not meet the slow wave amplitude criteria. This supports the abovementioned conclusion that the spindles detected in the slow waves were fast spindles and therefore they were mainly located at the positive peak of the slow wave, even though the spindle detection algorithm did include the whole sleep spindle frequency range (11–16 Hz). This may be explained by the fact that the spindle location is more likely to be at the positive peak of the slow wave in young adults [17]. Since age has been found to affect the shape of the spindle [46, 75] and the shape of the spindle has been found to become more even with age [75], it is likely that the spindle detection algorithm was able to mainly detect fast spindles. Thus the slight differences between the slow wave-locked and spindle-locked approaches may result from the spindle-detection algorithm focusing more on the exact spindle shape unlike the HT or complex demodulation.

Age plays a large part in the characterization of sleep spindles. Sleep spindle amplitude has been found to decrease, causing the spindles to lose their shape with age [46, 75]. Hence, the amplitude for the duration of the spindle becomes more even with age [75]. Therefore, this might lead to differences in results from different analysis methods, as methods such as complex demodulation can pick up more spindle shapes from flatter spindles. Furthermore, this may result in missing possible spindles in the spindle detection algorithm, when it is used to analyze a group of patients with varying ages.

Age plays a part in slow wave detection as well. It has been shown that the amplitude of slow wave sleep decreases in older subjects [76]. Therefore, comparing results of different studies that have dissimilar slow wave detection criteria, can be challenging. Since the detection methods often rely on amplitude thresholding, the threshold values between different methods can be very different, depending on which age demographic they have been developed on. The slow wave detection method which was implemented in this study, has been utilized previously in [26] with a threshold for detecting slow half waves being -80 µV. In other studies, the threshold for slow half wave detection has varied broadly. Papalambros et al. used -40 µV in their study [77] and Schneider et al. used mainly -80 µV threshold in their study, but they adapted the thresholds to -50 µV or -60 µV in some cases [78]. Furthermore, the challenge with threshold-based methods is that they tend to be susceptible to marking artefacts as slow waves and therefore result in off-target recognition [79]. However, in this study, this was avoided by removing any EEG waves which had an amplitude higher than the normal EEG amplitude range.

This study included some limitations that need to be considered. One of these was that the study population consisted of patients of different ages. As already mentioned, the age has an effect on spindle shape [46, 75] as well as the location of the spindle [17]. Furthermore, age has been reported to have an effect on slow wave amplitude [15]. Therefore, choosing a demographic within set age range is beneficial. Additionally, the lowpass filter before downsampling had a higher threshold for filtering that was required by the Nyquist theorem. Therefore, the results may still include errors due to the aliasing effect. Furthermore, the study population consisted of patients with suspected sleep apnea. Therefore, the results obtained in this thesis do not reflect the healthy population. However, this study focused on comparing different analysis methods and the aim was to include as much data as possible, and thus, dividing the data by age was not essential. Furthermore, the definition of a slow wave depends on the study [77, 78] and therefore, studies utilizing a different definition for a slow wave will not be comparable with this study. Additionally, only one channel was used in this study. Slow spindle and slow wave frequencies have been detected mainly in the fronto-central derivations, while fast spindles have been detected more in the centro-parietal derivations [24]. Therefore, the central channel C4-M1 was selected in this study to obtain the whole sleep spindle frequency range (11–16 Hz). However, the possible mixture of slow and fast spindles originating from different parts of the brain most likely had an effect on the results.

9 Conclusions

Time synchronization between sleep spindles and slow wave oscillation was found in this study using both the HT and complex demodulation. The coupling of these two EEG patterns was observed to be the strongest at the ascending slope and around the positive peak of the slow wave. Weaker coupling between these two wave patterns was observed at the descending slope of the slow wave. These observations were supported by the results from both datasets. Furthermore, for the slow wave-locked approach the used analysis method did not show any major differences. Both the complex demodulation and the HT performed similarly. As for the spindle-locked approach, the results showed that both complex demodulation and HT performed comparably as well. Additionally, the spindle detection algorithm was found to agree with the spindle location obtained using complex demodulation.

References

[1] D. B. Kirsch. "There and back again: A current history of sleep medicine". In: *Chest* 139.4 (2011), pp. 939–946.

[2] M. Hirshkowitz. "The History of Polysomnography: Tool of Scientific Discovery". In: *Sleep Medicine*. Ed. by S. Chokroverty and M Billiard. 1st. New York: Springer, 2015, pp. 91–100.

[3] H. Berger. "Über das Elektrenkephalogramm des Menschen - Dritte Mitteilung". In: *Archiv für Psychiatrie und Nervenkrankheiten* 87 (1929), pp. 527–570.

[4] A. L. Loomis, E. Newton Harvey, and G. Hobart. "Potential rhythms of the cerebral cortex during sleep". In: *Science* 81.2111 (1935), pp. 597–598.

[5] A. Kales and A. Rechtschaffen. *A Manual of Standardized Terminology, Techniques and Scoring System for Sleep Stages of Human Subjects: Allan Rechtschaffen and Anthony Kales, Editors*. 1968.

[6] C. Iber et al. *The AASM Manual for the Scoring of Sleep and Associated Events: Rules, Terminology and Technical Specifications*. Westchester, 2007.

[7] M. M. Troester, S. F. Quan, and R. B. Berry. *The AASM Manual for the Scoring of Sleep and Associated Events: Rules, Terminology and Technical Specifications*. Darien, 2023.

[8] M. J. Blake et al. "Adolescent-Sleep-Intervention Research: Current State and Future Directions". In: *Current Directions in Psychological Science* 28.5 (2019), pp. 475–482.

[9] E. S. Bruce, L. Lunt, and J. E. McDonagh. "Sleep in adolescents and young adults". In: *Clinical medicine (London, England)* 17.5 (2017), pp. 424–4228.

[10] M. Schlieber and J. Han. "The Role of Sleep in Young Children's Development: A Review". In: *The Journal of genetic psychology* 182.4 (2021), pp. 205–217.

[11] E. R. Kandel et al. *Principles of Neural Science*. Ed. by Anne Sydor and Harriet Lebowitz. 5th. McGraw-Hill Companies, 2013.

[12] H. P. A. Van Dongen et al. "The cumulative cost of additional wakefulness: Dose-response effects on neurobehavioral functions and sleep physiology from chronic sleep restriction and total sleep deprivation". In: *Sleep* 26.2 (2003), pp. 117–126.

[13] M. A. Grandner et al. "Mortality associated with short sleep duration: The evidence, the possible mechanisms, and the future". In: *Sleep Medicine Reviews* 14.3 (2010), pp. 191–203.

[14] S. Chokroverty. "Overview of sleep & sleep disorders". In: *The Indian journal of medical research* 131 (2010), pp. 126–140.

[15] I. M. Colrain. "The K-Complex: A 7-Decade History". In: *Sleep* 28.2 (2005), pp. 255–273.

[16] Z. Clemens et al. "Temporal coupling of parahippocampal ripples, sleep spindles and slow oscillations in humans". In: *Brain* 130.11 (2007), pp. 2868–2878.

[17] R. F. Helfrich et al. “Old Brains Come Uncoupled in Sleep: Slow Wave-Spindle Synchrony, Brain Atrophy, and Forgetting”. In: *Neuron* 97.1 (2018), pp. 221–230.

[18] S. C. Warby et al. “Sleep-spindle detection: crowdsourcing and evaluating performance of experts, non-experts and automated methods”. In: *Nature Methods* 11.4 (2014), pp. 385–392.

[19] E. Huupponen et al. “Development and comparison of four sleep spindle detection methods”. In: *Artificial Intelligence in Medicine* 40.3 (2007), pp. 157–170.

[20] V. V. Grubov et al. “Recognizing of stereotypic patterns in epileptic EEG using empirical modes and wavelets”. In: *Physica A: Statistical Mechanics and its Applications* 486 (2017), pp. 206–217.

[21] A. Tsanas and G. D. Clifford. “Stage-independent, single lead EEG sleep spindle detection using the continuous wavelet transform and local weighted smoothing”. In: *Frontiers in Human Neuroscience* 9.181 (2015).

[22] E. Ventouras et al. “Amplitude normalization applied to an artificial neural network-based automatic sleep spindle detection system”. In: *2014 36th Annual International Conference of the IEEE Engineering in Medicine and Biology Society* (2014), pp. 3240–3243.

[23] T. Andrillon et al. “Sleep Spindles in Humans: Insights from Intracranial EEG and Unit Recordings”. In: *The Journal of Neuroscience* 31.49 (2011), p. 17821.

[24] M. Mölle et al. “Fast and Slow Spindles during the Sleep Slow Oscillation: Disparate Coalescence and Engagement in Memory Processing”. In: *Sleep* 34.10 (2011), pp. 1411–1421.

[25] B. E Muehlroth et al. “Precise Slow Oscillation–Spindle Coupling Promotes Memory Consolidation in Younger and Older Adults”. In: *Scientific Reports* 9.1 (2019), p. 1940.

[26] J. Yordanova et al. “Dynamic coupling between slow waves and sleep spindles during slow wave sleep in humans is modulated by functional pre-sleep activation”. In: *Scientific Reports* 7.1 (2017).

[27] F. Lopes da Silva. “EEG and MEG: Relevance to neuroscience”. In: *Neuron* 80.5 (2013), pp. 1112–1128.

[28] T. Kirschstein and R. Köhling. “What is the Source of the EEG?” In: *Clinical EEG and Neuroscience* 40.3 (2009), pp. 146–149.

[29] J. Malmivuo and R. Plonsey. *Bioelectromagnetism - Principles and Applications of Bioelectric and Biomagnetic Fields*. New York: Oxford University Press, 1995.

[30] M. Soufineyestani, D. Dowling, and A. Khan. “Electroencephalography (EEG) Technology Applications and Available Devices”. In: *Applied Sciences* 10.21 (2020).

[31] J. N. Acharya et al. “American Clinical Neurophysiology Society Guideline 2: Guidelines for Standard Electrode Position Nomenclature”. In: *Journal of Clinical Neurophysiology* 33.4 (2016).

[32] L. F. Nicolas-Alonso and J. Gomez-Gil. “Brain computer interfaces, a review”. In: *Sensors* 12.2 (2012), pp. 1211–1279.

[33] N. Padfield et al. “EEG-based brain-computer interfaces using motor-imagery: Techniques and challenges”. In: *Sensors (Switzerland)* 19.6 (2019).

[34] A. Perrottelli et al. “EEG-Based Measures in At-Risk Mental State and Early Stages of Schizophrenia: A Systematic Review”. In: *Frontiers in Psychiatry* 12 (2021).

[35] N. Baranwal, P. K. Yu, and N. S. Siegel. “Sleep physiology, pathophysiology, and sleep hygiene”. In: *Progress in Cardiovascular Diseases* 77 (2023), pp. 59–69.

[36] R. Stickgold. “Sleep-dependent memory consolidation”. In: *Nature* 437 (2005), pp. 1272–1278.

[37] M. Hirshkowitz. “Methodology”. In: *Principles and Practice of Sleep Medicine*. Ed. by Mary Carskadon and Allan Rechtschaffen. 4th. Philadelphia: Elsevier, 2005. Chap. 17, pp. 1359–1377.

[38] P. R. Carney and J. D. Geyer. *Atlas of polysomnography*. 3rd. Wolters Kluwer, 2018.

[39] X. Tan et al. “A narrative review of interventions for improving sleep and reducing circadian disruption in medical inpatients”. In: *Sleep Medicine* 59 (2019), pp. 42–50.

[40] L. M. J. Fernandez and A. Lüthi. “Sleep Spindles: Mechanisms and Functions”. In: *Physiological Reviews* 100.2 (2020), pp. 805–868.

[41] J. S. Zygierewicz et al. “High resolution study of sleep spindles”. In: *Clinical Neurophysiology* 110.12 (1999), pp. 2136–2147.

[42] K. Schiller et al. “Focal epilepsy disrupts spindle structure and function”. In: *Scientific Reports* 12.1 (2022), p. 11137.

[43] D. S. Manoach et al. “Reduced Sleep Spindles in Schizophrenia: A Treatable Endophenotype That Links Risk Genes to Impaired Cognition?” In: *Biological Psychiatry* 80.8 (2016), pp. 599–608.

[44] M. M. Grigg-Damberger and N. Foldvary-Schaefer. “Sleep Biomarkers Help Predict the Development of Alzheimer Disease”. In: *Journal of Clinical Neurophysiology* 39.5 (2022), pp. 327–334.

[45] M. M. Grigg-Damberger, O. Hussein, and T. Kulik. “Sleep Spindles and K-Complexes Are Favorable Prognostic Biomarkers in Critically Ill Patients”. In: *Journal of Clinical Neurophysiology* 39.5 (2022), pp. 372–382.

[46] F. A. Gibbs and E. L. Gibbs. *Atlas of Electroencephalography*. 2nd. Cambridge: Addison Wesley Press, 1950.

[47] M. Jobert et al. “Topographical analysis of sleep spindle activity”. In: *Neuropsychobiology* 26.4 (1992), pp. 210–217.

[48] E. Werth et al. “Spindle frequency activity in the sleep EEG: individual differences and topographical distribution”. In: *Electroencephalography and Clinical Neurophysiology* 103.5 (1997), pp. 535–542.

[49] A. Lüthi. “Sleep Spindles: Where They Come From, What They Do”. In: *The Neuroscientist* 20.3 (2014), pp. 243–256.

[50] M. Steriade et al. “The deafferented reticular thalamic nucleus generates spindle rhythmicity”. In: *Journal of Neurophysiology* 57.1 (1987), pp. 260–273.

[51] H. Alsolai et al. “A Systematic Review of Literature on Automated Sleep Scoring”. In: *IEEE Access* 10 (2022), pp. 79419–79443.

[52] L. Genzel et al. “Light sleep versus slow wave sleep in memory consolidation: A question of global versus local processes?” In: *Trends in Neurosciences* 37.1 (2014), pp. 10–19.

[53] D. Léger et al. “Slow-wave sleep: From the cell to the clinic”. In: *Sleep Medicine Reviews* 41 (2018), pp. 113–132.

[54] G. T. Neske. “The Slow Oscillation in Cortical and Thalamic Networks: Mechanisms and Functions”. In: *Frontiers in Neural Circuits* 9 (2016).

[55] M. Murphy et al. “Source modeling sleep slow waves”. In: *Proceedings of the National Academy of Sciences* 106.5 (2009), pp. 1608–1613.

[56] I. Timofeev et al. “Origin of Slow Cortical Oscillations in Deafferented Cortical Slabs”. In: *Cerebral Cortex* 10.12 (2000), pp. 1185–1199.

[57] M. Massimini et al. “The Sleep Slow Oscillation as a Traveling Wave”. In: *The Journal of Neuroscience* 24.31 (2004), p. 6862.

[58] A. W. Varga et al. “Effects of aging on slow-wave sleep dynamics and human spatial navigational memory consolidation”. In: *Neurobiology of Aging* 42 (2016), pp. 142–149.

[59] Y. F. Lee et al. “Slow Wave Sleep Is a Promising Intervention Target for Alzheimer’s Disease”. In: *Frontiers in Neuroscience* 14 (2020), p. 705.

[60] J. Beck, M. J. Cordi, and B. Rasch. “Hypnotic Suggestions Increase Slow-Wave Parameters but Decrease Slow-Wave Spindle Coupling”. In: *Nature and Science of Sleep* 13 (2021), pp. 1383–1393.

[61] M. Niknazar et al. “Coupling of Thalamocortical Sleep Oscillations Are Important for Memory Consolidation in Humans”. In: *PLOS ONE* 10.12 (2015).

[62] N. E. Huang et al. “The Empirical Mode Decomposition and the Hilbert Spectrum for Nonlinear and Non-Stationary Time Series Analysis”. In: *Proceedings: Mathematical, Physical and Engineering Sciences* 454.1971 (1998), pp. 903–995.

[63] S. Maheshwari, A. Kumar, and M. Tech. “Empirical Mode Decomposition: Theory and Applications”. In: *International Journal of Electronic and Electrical Engineering* 7.8 (2014), pp. 873–878.

[64] E. Foufoula-Georgiou and P. Kumar. *Wavelets in Geophysics*. 1st. Vol. 4. San Diego: Academic Press, 1994.

[65] S. Mallat. *A Wavelet Tour of Signal Processing: The Sparse Way*. 3rd. Academic Press, 2008.

[66] I. Daubechies. *Ten Lectures on Wavelets*. Vol. 61. Philadelphia: SIAM, 1992.

[67] L. Aguiar-Conraria and M. J. Soares. *The continuous wavelet transform: A primer*. Tech. rep. 2011.

[68] R. B. Govindan et al. “Understanding dynamics of the system using Hilbert phases: An application to study neonatal and fetal brain signals”. In: *Physical Review E* 80.4 (2009).

[69] A. Singh. “Survey Paper on Hilbert Transform With its Applications in Signal Processing”. In: *International Journal of Computer Science and Information Technologies* 5.3 (2014), pp. 3880–3882.

[70] R. G. Lyons. *Understanding Digital Signal Processing*. 2nd. Bernard Goodwin, 2004.

[71] P. Y. Ktonas and N. Papp. “Instantaneous envelope and phase extraction from real signals: Theory, implementation, and an application to EEG analysis”. In: *Signal Processing* 2.4 (1980), pp. 373–385.

[72] S. K. Yoo and H. C. Kang. “Amplitude and Phase Analysis of EEG Signal by Complex Demodulation”. In: *International Journal of Biomedical and Biological Engineering* 7.10 (2013), pp. 648–651.

[73] Y. L. Hao, Y. Ueda, and N. Ishii. “Improved procedure of complex demodulation and an application to frequency analysis of sleep spindles in EEG”. In: *Medical and Biological Engineering and Computing* 30.4 (1992), pp. 406–412.

[74] T. T. Dang-Vu et al. “Spontaneous neural activity during human slow wave sleep”. In: *Proceedings of the National Academy of Sciences* 105.39 (2008), pp. 15160–15165.

[75] J. C. Principe and J. R. Smith. “Sleep Spindle Characteristics as a Function of Age”. In: *Sleep* 5.1 (1982), pp. 73–84.

[76] I. M. Colrain et al. “Sleep evoked delta frequency responses show a linear decline in amplitude across the adult lifespan”. In: *Neurobiology of Aging* 31.5 (2010), pp. 874–883.

[77] N. A. Papalambros et al. “Acoustic enhancement of sleep slow oscillations and concomitant memory improvement in older adults”. In: *Frontiers in Human Neuroscience* 11 (2017).

[78] J. Schneider et al. “Susceptibility to auditory closed-loop stimulation of sleep slow oscillations changes with age”. In: *Sleep* 43.12 (2020).

[79] M. Wunderlin et al. “Automatized online prediction of slow-wave peaks during non-rapid eye movement sleep in young and old individuals: Why we should not always rely on amplitude thresholds”. In: *Journal of Sleep Research* 31.6 (2022).